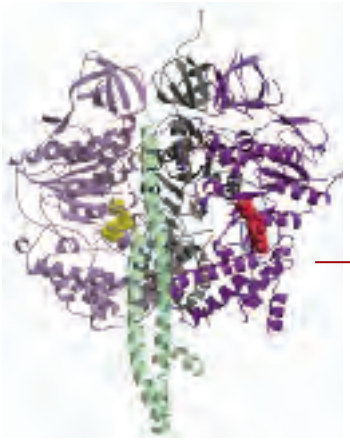

chapter 19

OXIDATIVE PHOSPHORYLATION AND PHOTOPHOSPHORYLATION

If an idea presents itself to us, we must not reject it simply because it does not agree with the logical deductions of a reigning theory.

—*Claude Bernard,* An Introduction to the Study of Experimental Medicine, *1813*

The aspect of the present position of consensus that I find most remarkable and admirable, is the altruism and generosity with which former opponents of the chemiosmotic hypothesis have not only come to accept it, but have actively promoted it to the status of a theory.

—*Peter Mitchell, Nobel Address, 1978*

Oxidative phosphorylation is the culmination of energy-yielding metabolism in aerobic organisms. All oxidative steps in the degradation of carbohydrates, fats, and amino acids converge at this final stage of cellular respiration, in which the energy of oxidation drives the synthesis of ATP. Photophosphorylation is the means by which photosynthetic organisms capture the energy of sunlight—the ultimate source of energy in the biosphere—and harness it to make ATP. Together, oxidative phosphorylation and photophosphorylation account for most of the ATP synthesized by most organisms most of the time.

In eukaryotes, oxidative phosphorylation occurs in mitochondria, photophosphorylation in chloroplasts. Oxidative phosphorylation involves the *reduction* of O_2 to H_2O with electrons donated by NADH and $FADH_2$; it occurs equally well in light or darkness. Photophosphorylation involves the *oxidation* of H_2O to O_2, with $NADP^+$ as ultimate electron acceptor; it is absolutely dependent on the energy of light. Despite their differences, these two highly efficient energy-converting processes have fundamentally similar mechanisms.

Our current understanding of ATP synthesis in mitochondria and chloroplasts is based on the hypothesis, introduced by Peter Mitchell in 1961, that transmembrane differences in proton concentration are the reservoir for the energy extracted from biological oxidation reactions. This **chemiosmotic theory** has been accepted as one of the great unifying principles of twentieth century biology. It provides insight into the processes of oxidative phosphorylation and photophosphorylation, and into such apparently disparate energy transductions as active transport across membranes and the motion of bacterial flagella.

Oxidative phosphorylation and photophosphorylation are mechanistically similar in three respects. (1) Both

processes involve the flow of electrons through a chain of membrane-bound carriers. (2) The free energy made available by this "downhill" (exergonic) electron flow is coupled to the "uphill" transport of protons across a proton-impermeable membrane, conserving the free energy of fuel oxidation as a transmembrane electrochemical potential (p. 391). (3) The transmembrane flow of protons down their concentration gradient through specific protein channels provides the free energy for synthesis of ATP, catalyzed by a membrane protein complex (ATP synthase) that couples proton flow to phosphorylation of ADP.

We begin this chapter with oxidative phosphorylation. We first describe the components of the electron-transfer chain, their organization into large functional complexes in the inner mitochondrial membrane, the path of electron flow through them, and the proton movements that accompany this flow. We then consider the remarkable enzyme complex that, by "rotational catalysis," captures the energy of proton flow in ATP, and the regulatory mechanisms that coordinate oxidative phosphorylation with the many catabolic pathways by which fuels are oxidized. With this understanding of mitochondrial oxidative phosphorylation, we turn to photophosphorylation, looking first at the absorption of light by photosynthetic pigments, then at the light-driven flow of electrons from H_2O to $NADP^+$ and the molecular basis for coupling electron and proton flow. We also consider the similarities of structure and mechanism between the ATP synthases of chloroplasts and mitochondria, and the evolutionary basis for this conservation of mechanism.

OXIDATIVE PHOSPHORYLATION

19.1 Electron-Transfer Reactions in Mitochondria

The discovery in 1948 by Eugene Kennedy and Albert Lehninger that mitochondria are the site of oxidative phosphorylation in eukaryotes marked the beginning of the modern phase of studies in biological energy transductions. Mitochondria, like gram-negative bacteria, have two membranes (Fig. 19–1). The outer mitochondrial membrane is readily permeable to small molecules (M_r <5,000) and ions, which move freely through transmembrane channels formed by a family of integral membrane proteins called porins. The inner membrane is impermeable to most small molecules and ions, including protons (H^+); the only species that cross this membrane do so through specific transporters. The inner membrane bears the components of the respiratory chain and the ATP synthase.

Albert L. Lehninger, 1917–1986

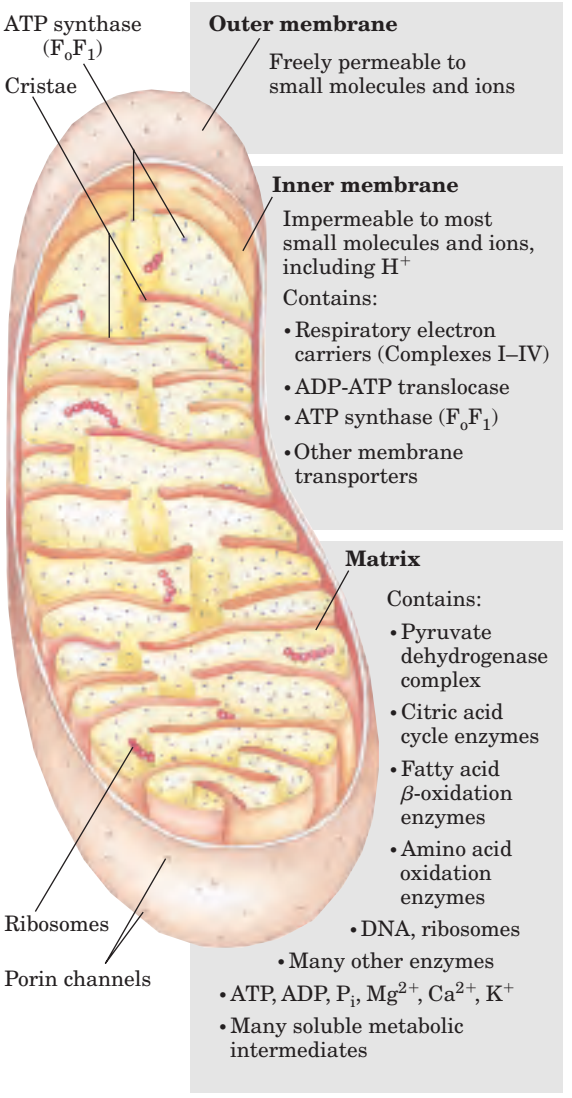

FIGURE 19–1 Biochemical anatomy of a mitochondrion. The convolutions (cristae) of the inner membrane provide a very large surface area. The inner membrane of a single liver mitochondrion may have more than 10,000 sets of electron-transfer systems (respiratory chains) and ATP synthase molecules, distributed over the membrane surface. Heart mitochondria, which have more profuse cristae and thus a much larger area of inner membrane, contain more than three times as many sets of electron-transfer systems as liver mitochondria. The mitochondrial pool of coenzymes and intermediates is functionally separate from the cytosolic pool. The mitochondria of invertebrates, plants, and microbial eukaryotes are similar to those shown here, but with much variation in size, shape, and degree of convolution of the inner membrane.

The mitochondrial matrix, enclosed by the inner membrane, contains the pyruvate dehydrogenase complex and the enzymes of the citric acid cycle, the fatty

acid β-oxidation pathway, and the pathways of amino acid oxidation—all the pathways of fuel oxidation except glycolysis, which takes place in the cytosol. The selectively permeable inner membrane segregates the intermediates and enzymes of cytosolic metabolic pathways from those of metabolic processes occurring in the matrix. However, specific transporters carry pyruvate, fatty acids, and amino acids or their α-keto derivatives into the matrix for access to the machinery of the citric acid cycle. ADP and P_i are specifically transported into the matrix as newly synthesized ATP is transported out.

Electrons Are Funneled to Universal Electron Acceptors

Oxidative phosphorylation begins with the entry of electrons into the respiratory chain. Most of these electrons arise from the action of dehydrogenases that collect electrons from catabolic pathways and funnel them into universal electron acceptors—nicotinamide nucleotides (NAD^+ or $NADP^+$) or flavin nucleotides (FMN or FAD).

Nicotinamide nucleotide–linked dehydrogenases catalyze reversible reactions of the following general types:

$$\text{Reduced substrate} + NAD^+ \rightleftharpoons \text{oxidized substrate} + NADH + H^+$$

$$\text{Reduced substrate} + NADP^+ \rightleftharpoons \text{oxidized substrate} + NADPH + H^+$$

Most dehydrogenases that act in catabolism are specific for NAD^+ as electron acceptor (Table 19–1). Some are in the cytosol, others are in mitochondria, and still others have mitochondrial and cytosolic isozymes.

NAD-linked dehydrogenases remove two hydrogen atoms from their substrates. One of these is transferred as a hydride ion ($:H^-$) to NAD^+; the other is released as H^+ in the medium (see Fig. 13–15). NADH and NADPH are water-soluble electron carriers that associate *reversibly* with dehydrogenases. NADH carries electrons from catabolic reactions to their point of entry into the respiratory chain, the NADH dehydrogenase complex described below. NADPH generally supplies electrons to anabolic reactions. Cells maintain separate pools of NADPH and NADH, with different redox potentials. This is accomplished by holding the ratios of [reduced form]/[oxidized form] relatively high for NADPH and relatively low for NADH. Neither NADH nor NADPH can cross the inner mitochondrial membrane, but the electrons they carry can be shuttled across indirectly, as we shall see.

Flavoproteins contain a very tightly, sometimes covalently, bound flavin nucleotide, either FMN or FAD (see Fig. 13–18). The oxidized flavin nucleotide can accept either one electron (yielding the semiquinone form) or two (yielding $FADH_2$ or $FMNH_2$). Electron transfer occurs because the flavoprotein has a higher reduction potential than the compound oxidized. The standard reduction potential of a flavin nucleotide, unlike that of NAD or NADP, depends on the protein with which it is associated. Local interactions with functional groups in the protein distort the electron orbitals in the flavin ring, changing the relative stabilities of oxidized and reduced forms. The relevant standard reduction

TABLE 19–1 Some Important Reactions Catalyzed by NAD(P)H-Linked Dehydrogenases

Reaction[*]	*Location*[†]
NAD-linked	
α-Ketoglutarate + CoA + NAD^+ ⇌ succinyl-CoA + CO_2 + NADH + H^+	M
L-Malate + NAD^+ ⇌ oxaloacetate + NADH + H^+	M and C
Pyruvate + CoA + NAD^+ ⇌ acetyl-CoA + CO_2 + NADH + H^+	M
Glyceraldehyde 3-phosphate + P_i + NAD^+ ⇌ 1,3-bisphosphoglycerate + NADH + H^+	C
Lactate + NAD^+ ⇌ pyruvate + NADH + H^+	C
β-Hydroxyacyl-CoA + NAD^+ ⇌ β-ketoacyl-CoA + NADH + H^+	M
NADP-linked	
Glucose 6-phosphate + $NADP^+$ ⇌ 6-phosphogluconate + NADPH + H^+	C
NAD- or NADP-linked	
L-Glutamate + H_2O + $NAD(P)^+$ ⇌ α-ketoglutarate + NH_4^+ + NAD(P)H	M
Isocitrate + $NAD(P)^+$ ⇌ α-ketoglutarate + CO_2 + NAD(P)H + H^+	M and C

[*] These reactions and their enzymes are discussed in Chapters 14 through 18.
[†] M designates mitochondria; C, cytosol.

potential is therefore that of the particular flavoprotein, not that of isolated FAD or FMN. The flavin nucleotide should be considered part of the flavoprotein's active site rather than a reactant or product in the electron-transfer reaction. Because flavoproteins can participate in either one- or two-electron transfers, they can serve as intermediates between reactions in which two electrons are donated (as in dehydrogenations) and those in which only one electron is accepted (as in the reduction of a quinone to a hydroquinone, described below).

Electrons Pass through a Series of Membrane-Bound Carriers

The mitochondrial respiratory chain consists of a series of sequentially acting electron carriers, most of which are integral proteins with prosthetic groups capable of accepting and donating either one or two electrons. Three types of electron transfers occur in oxidative phosphorylation: (1) direct transfer of electrons, as in the reduction of Fe^{3+} to Fe^{2+}; (2) transfer as a hydrogen atom ($H^+ + e^-$); and (3) transfer as a hydride ion ($:H^-$), which bears two electrons. The term **reducing equivalent** is used to designate a single electron equivalent transferred in an oxidation-reduction reaction.

In addition to NAD and flavoproteins, three other types of electron-carrying molecules function in the respiratory chain: a hydrophobic quinone (ubiquinone) and two different types of iron-containing proteins (cytochromes and iron-sulfur proteins). **Ubiquinone** (also called **coenzyme Q,** or simply **Q**) is a lipid-soluble benzoquinone with a long isoprenoid side chain (Fig. 19–2). The closely related compounds plastoquinone (of plant chloroplasts) and menaquinone (of bacteria) play roles analogous to that of ubiquinone, carrying electrons in membrane-associated electron-transfer chains. Ubiquinone can accept one electron to become the semiquinone radical ($^{\bullet}QH$) or two electrons to form ubiquinol (QH_2) (Fig. 19–2) and, like flavoprotein carriers, it can act at the junction between a two-electron donor and a one-electron acceptor. Because ubiquinone is both small and hydrophobic, it is freely diffusible within the lipid bilayer of the inner mitochondrial membrane and can shuttle reducing equivalents between other, less mobile electron carriers in the membrane. And because it carries both electrons and protons, it plays a central role in coupling electron flow to proton movement.

The **cytochromes** are proteins with characteristic strong absorption of visible light, due to their iron-containing heme prosthetic groups (Fig. 19–3). Mitochondria contain three classes of cytochromes, designated *a, b,* and *c,* which are distinguished by differences in their light-absorption spectra. Each type of cytochrome in its reduced (Fe^{2+}) state has three absorption bands in the visible range (Fig. 19–4). The longest-wavelength band is near 600 nm in type *a* cytochromes,

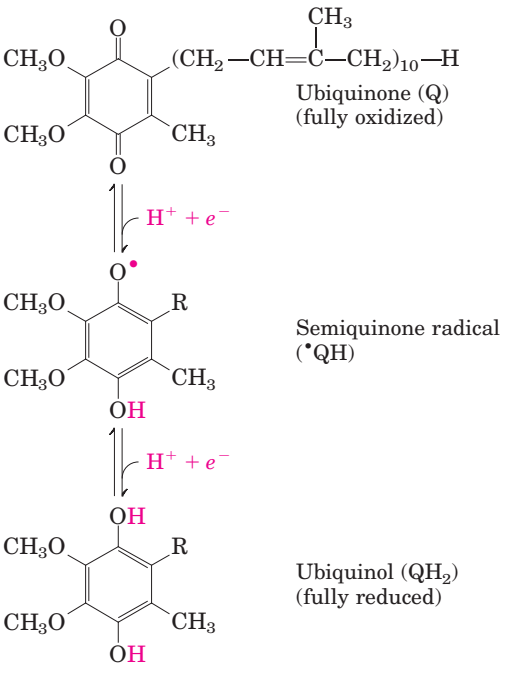

FIGURE 19–2 Ubiquinone (Q, or coenzyme Q). Complete reduction of ubiquinone requires two electrons and two protons, and occurs in two steps through the semiquinone radical intermediate.

near 560 nm in type *b,* and near 550 nm in type *c.* To distinguish among closely related cytochromes of one type, the exact absorption maximum is sometimes used in the names, as in cytochrome b_{562}.

The heme cofactors of *a* and *b* cytochromes are tightly, but not covalently, bound to their associated proteins; the hemes of *c*-type cytochromes are covalently attached through Cys residues (Fig. 19–3). As with the flavoproteins, the standard reduction potential of the heme iron atom of a cytochrome depends on its interaction with protein side chains and is therefore different for each cytochrome. The cytochromes of type *a* and *b* and some of type *c* are integral proteins of the inner mitochondrial membrane. One striking exception is the cytochrome *c* of mitochondria, a soluble protein that associates through electrostatic interactions with the outer surface of the inner membrane. We encountered cytochrome *c* in earlier discussions of protein structure (see Fig. 4–18).

Helmut Beinert

In **iron-sulfur proteins,** first discovered by Helmut Beinert, the iron is present not in heme but in association with inorganic sulfur atoms or with the sulfur atoms of Cys residues in the protein, or both. These iron-sulfur (Fe-S)

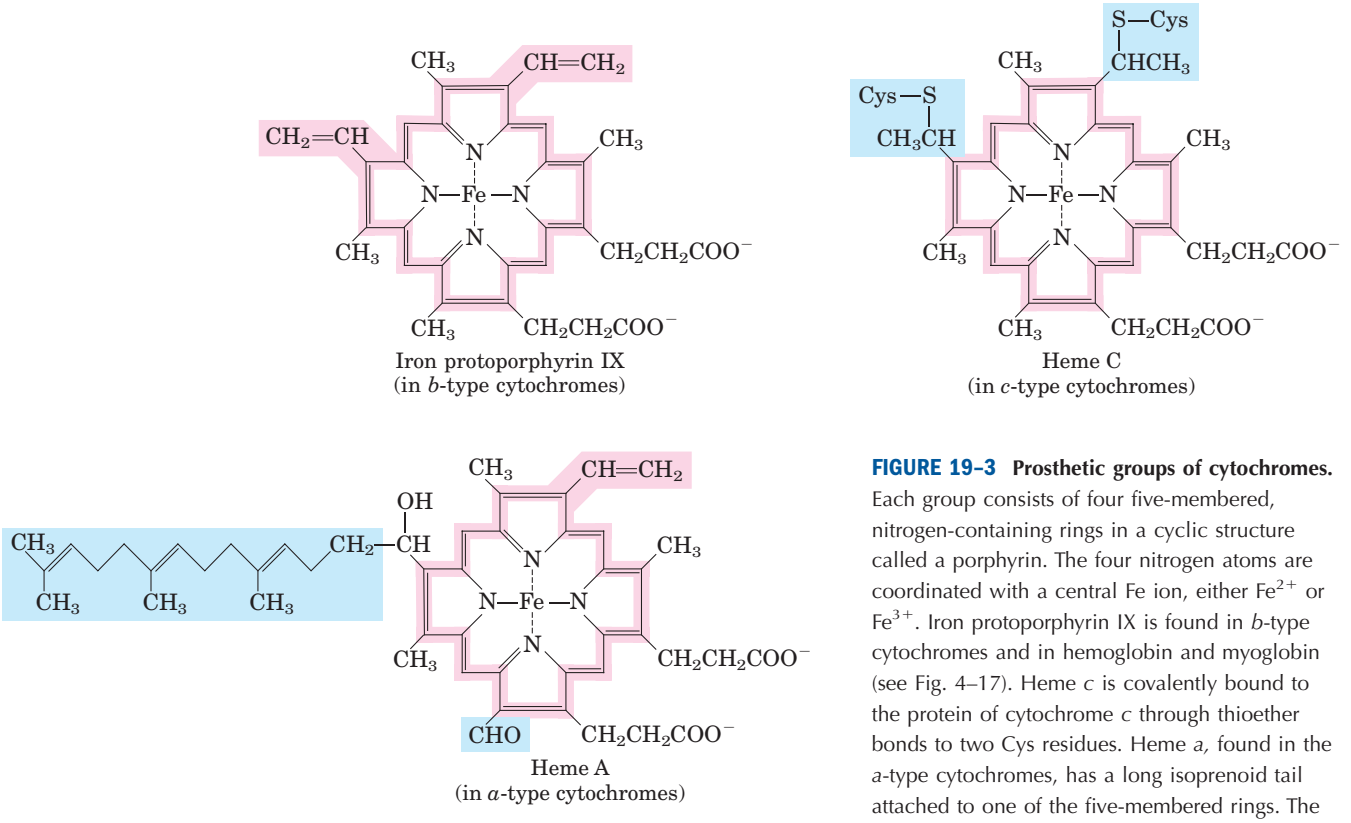

FIGURE 19–3 **Prosthetic groups of cytochromes.** Each group consists of four five-membered, nitrogen-containing rings in a cyclic structure called a porphyrin. The four nitrogen atoms are coordinated with a central Fe ion, either Fe^{2+} or Fe^{3+}. Iron protoporphyrin IX is found in *b*-type cytochromes and in hemoglobin and myoglobin (see Fig. 4–17). Heme *c* is covalently bound to the protein of cytochrome *c* through thioether bonds to two Cys residues. Heme *a,* found in the *a*-type cytochromes, has a long isoprenoid tail attached to one of the five-membered rings. The conjugated double-bond system (shaded pink) of the porphyrin ring accounts for the absorption of visible light by these hemes.

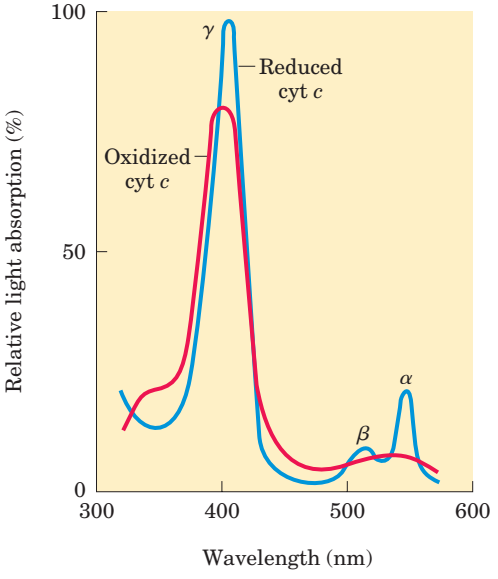

FIGURE 19–4 Absorption spectra of cytochrome *c* (cyt *c*) in its oxidized (red) and reduced (blue) forms. Also labeled are the characteristic α, β, and γ bands of the reduced form.

centers range from simple structures with a single Fe atom coordinated to four Cys —SH groups to more complex Fe-S centers with two or four Fe atoms (Fig. 19–5). **Rieske iron-sulfur proteins** (named after their discoverer, John S. Rieske) are a variation on this theme, in which one Fe atom is coordinated to two His residues rather than two Cys residues. All iron-sulfur proteins participate in one-electron transfers in which one iron atom of the iron-sulfur cluster is oxidized or reduced. At least eight Fe-S proteins function in mitochondrial electron transfer. The reduction potential of Fe-S proteins varies from −0.65 V to +0.45 V, depending on the microenvironment of the iron within the protein.

In the overall reaction catalyzed by the mitochondrial respiratory chain, electrons move from NADH, succinate, or some other primary electron donor through flavoproteins, ubiquinone, iron-sulfur proteins, and cytochromes, and finally to O_2. A look at the methods used to determine the sequence in which the carriers act is instructive, as the same general approaches have been used to study other electron-transfer chains, such as those of chloroplasts.

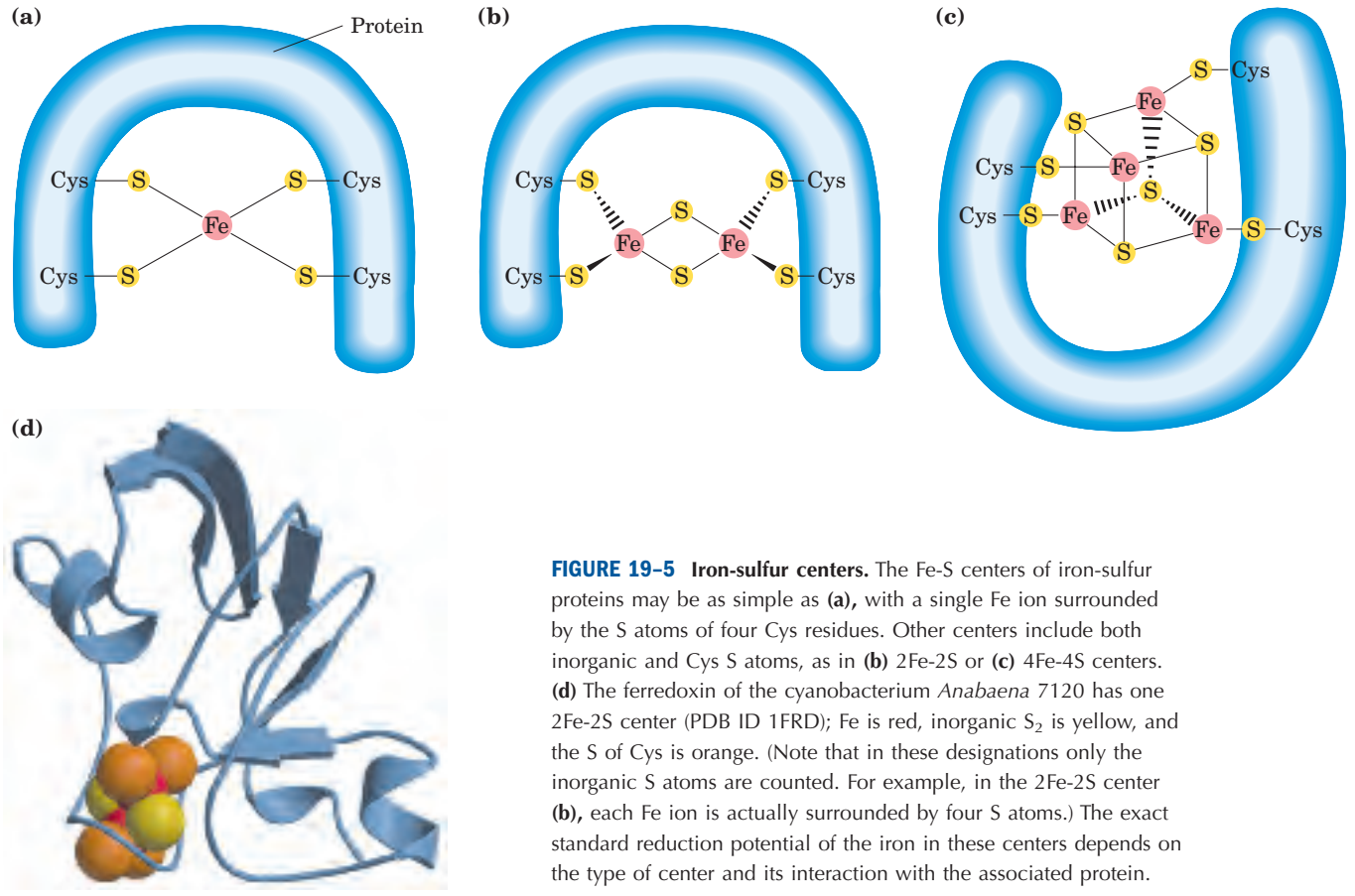

FIGURE 19–5 Iron-sulfur centers. The Fe-S centers of iron-sulfur proteins may be as simple as **(a),** with a single Fe ion surrounded by the S atoms of four Cys residues. Other centers include both inorganic and Cys S atoms, as in **(b)** 2Fe-2S or **(c)** 4Fe-4S centers. **(d)** The ferredoxin of the cyanobacterium *Anabaena* 7120 has one 2Fe-2S center (PDB ID 1FRD); Fe is red, inorganic S_2 is yellow, and the S of Cys is orange. (Note that in these designations only the inorganic S atoms are counted. For example, in the 2Fe-2S center **(b),** each Fe ion is actually surrounded by four S atoms.) The exact standard reduction potential of the iron in these centers depends on the type of center and its interaction with the associated protein.

First, the standard reduction potentials of the individual electron carriers have been determined experimentally (Table 19–2). We would expect the carriers to function in order of increasing reduction potential, because electrons tend to flow spontaneously from carriers of lower $E'°$ to carriers of higher $E'°$. The order of carriers deduced by this method is NADH → Q → cytochrome *b* → cytochrome c_1 → cytochrome *c* → cytochrome *a* → cytochrome a_3 → O_2. Note, however, that the order of standard reduction potentials is not necessarily the same as the order of *actual* reduction potentials under cellular conditions, which depend on the concentration of reduced and oxidized forms (p. 510). A second method for determining the sequence

TABLE 19–2 Standard Reduction Potentials of Respiratory Chain and Related Electron Carriers

Redox reaction (half-reaction)	*E'° (V)*
$2H^+ + 2e^- \longrightarrow H_2$	−0.414
$NAD^+ + H^+ + 2e^- \longrightarrow NADH$	−0.320
$NADP^+ + H^+ + 2e^- \longrightarrow NADPH$	−0.324
NADH dehydrogenase (FMN) + $2H^+ + 2e^- \longrightarrow$ NADH dehydrogenase ($FMNH_2$)	−0.30
Ubiquinone + $2H^+ + 2e^- \longrightarrow$ ubiquinol	0.045
Cytochrome *b* (Fe^{3+}) + $e^- \longrightarrow$ cytochrome *b* (Fe^{2+})	0.077
Cytochrome c_1 (Fe^{3+}) + $e^- \longrightarrow$ cytochrome c_1 (Fe^{2+})	0.22
Cytochrome *c* (Fe^{3+}) + $e^- \longrightarrow$ cytochrome *c* (Fe^{2+})	0.254
Cytochrome *a* (Fe^{3+}) + $e^- \longrightarrow$ cytochrome *a* (Fe^{2+})	0.29
Cytochrome a_3 (Fe^{3+}) + $e^- \longrightarrow$ cytochrome a_3 (Fe^{2+})	0.35
$\frac{1}{2}O_2 + 2H^+ + 2e^- \longrightarrow H_2O$	0.8166

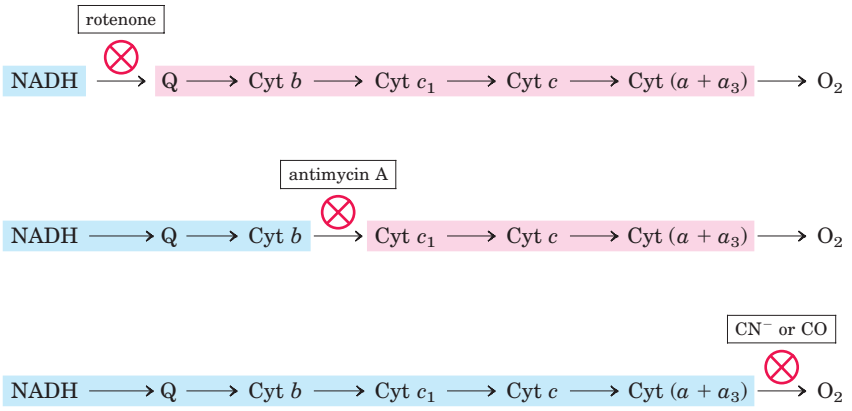

FIGURE 19–6 Method for determining the sequence of electron carriers. This method measures the effects of inhibitors of electron transfer on the oxidation state of each carrier. In the presence of an electron donor and O_2, each inhibitor causes a characteristic pattern of oxidized/reduced carriers: those before the block become reduced (blue), and those after the block become oxidized (pink).

of electron carriers involves reducing the entire chain of carriers experimentally by providing an electron source but no electron acceptor (no O_2). When O_2 is suddenly introduced into the system, the rate at which each electron carrier becomes oxidized (measured spectroscopically) reveals the order in which the carriers function. The carrier nearest O_2 (at the end of the chain) gives up its electrons first, the second carrier from the end is oxidized next, and so on. Such experiments have confirmed the sequence deduced from standard reduction potentials.

In a final confirmation, agents that inhibit the flow of electrons through the chain have been used in combination with measurements of the degree of oxidation of each carrier. In the presence of O_2 and an electron donor, carriers that function before the inhibited step become fully reduced, and those that function after this step are completely oxidized (Fig. 19–6). By using several inhibitors that block different steps in the chain, investigators have determined the entire sequence; it is the same as deduced in the first two approaches.

Electron Carriers Function in Multienzyme Complexes

The electron carriers of the respiratory chain are organized into membrane-embedded supramolecular complexes that can be physically separated. Gentle treatment of the inner mitochondrial membrane with detergents allows the resolution of four unique electron-carrier complexes, each capable of catalyzing electron transfer through a portion of the chain (Table 19–3; Fig. 19–7). Complexes I and II catalyze electron transfer to ubiquinone from two different electron donors: NADH (Complex I) and succinate (Complex II). Complex III carries electrons from reduced ubiquinone to cytochrome *c*, and Complex IV completes the sequence by transferring electrons from cytochrome *c* to O_2.

We now look in more detail at the structure and function of each complex of the mitochondrial respiratory chain.

Complex I: NADH to Ubiquinone Figure 19–8 illustrates the relationship between Complexes I and II and ubiquinone. **Complex I,** also called **NADH:ubiquinone oxidoreductase** or **NADH dehydrogenase,** is a large enzyme composed of 42 different polypeptide chains, including an FMN-containing flavoprotein and at least six iron-sulfur centers. High-resolution electron microscopy shows Complex I to be L-shaped, with one arm of the L in the membrane and the other extending into the matrix. As shown in Figure 19–9, Complex I catalyzes two simultaneous and obligately coupled processes: (1) the

TABLE 19–3 The Protein Components of the Mitochondrial Electron-Transfer Chain

Enzyme complex/protein	*Mass (kDa)*	*Number of subunits**	*Prosthetic group(s)*
I NADH dehydrogenase	850	43 (14)	FMN, Fe-S
II Succinate dehydrogenase	140	4	FAD, Fe-S
III Ubiquinone cytochrome *c* oxidoreductase	250	11	Hemes, Fe-S
Cytochrome *c*†	13	1	Heme
IV Cytochrome oxidase	160	13 (3–4)	Hemes; Cu_A, Cu_B

*Numbers of subunits in the bacterial equivalents in parentheses.
†Cytochrome *c* is not part of an enzyme complex; it moves between Complexes III and IV as a freely soluble protein.

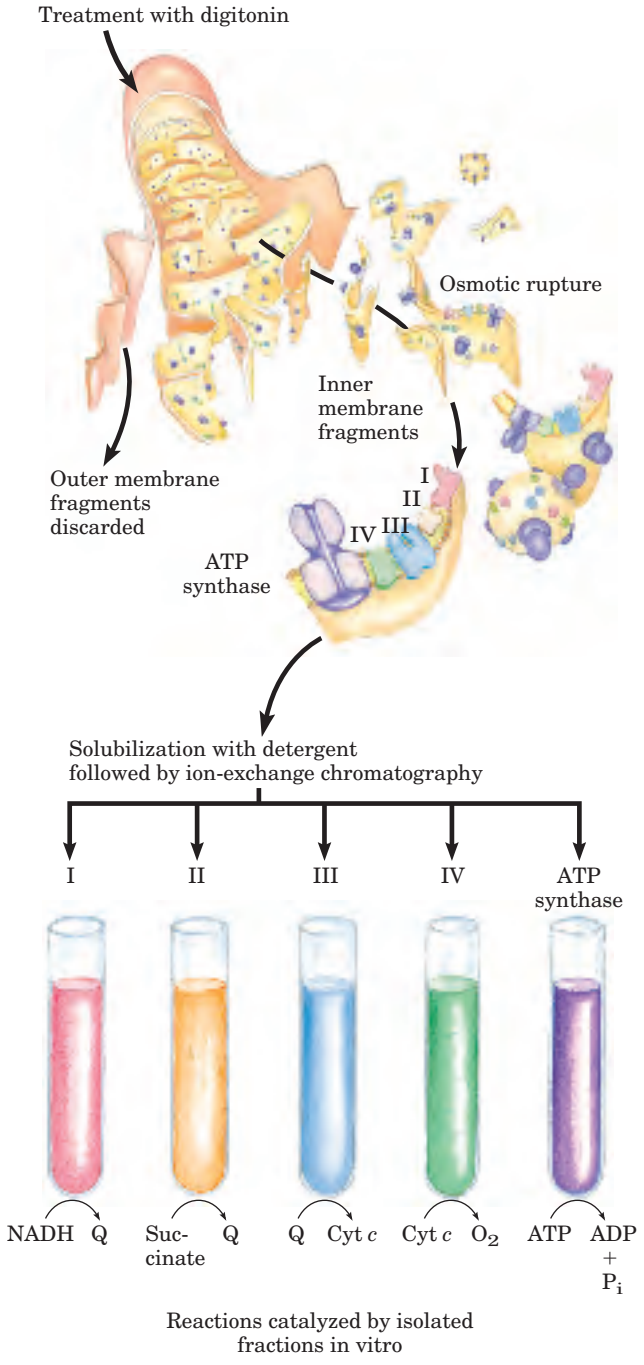

FIGURE 19–7 Separation of functional complexes of the respiratory chain. The outer mitochondrial membrane is first removed by treatment with the detergent digitonin. Fragments of inner membrane are then obtained by osmotic rupture of the mitochondria, and the fragments are gently dissolved in a second detergent. The resulting mixture of inner membrane proteins is resolved by ion-exchange chromatography into different complexes (I through IV) of the respiratory chain, each with its unique protein composition (see Table 19–3), and the enzyme ATP synthase (sometimes called Complex V). The isolated Complexes I through IV catalyze transfers between donors (NADH and succinate), intermediate carriers (Q and cytochrome *c*), and O_2, as shown. In vitro, isolated ATP synthase has only ATP-hydrolyzing (ATPase), not ATP-synthesizing, activity.

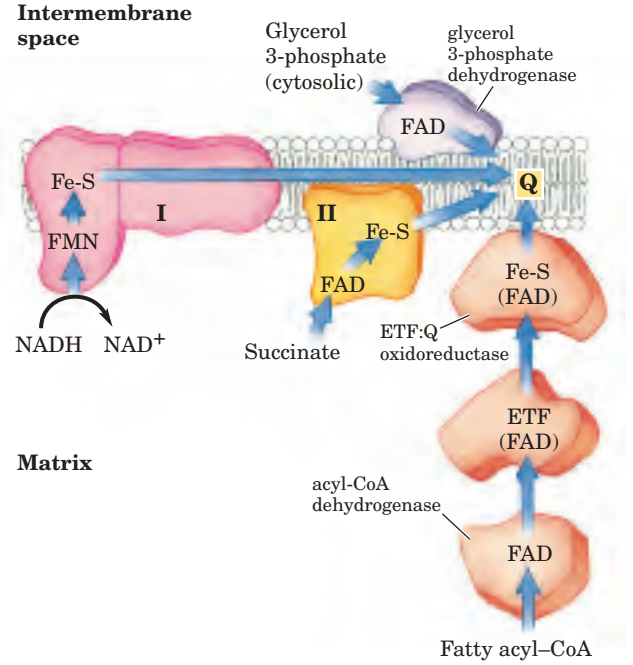

FIGURE 19–8 Path of electrons from NADH, succinate, fatty acyl–CoA, and glycerol 3-phosphate to ubiquinone. Electrons from NADH pass through a flavoprotein to a series of iron-sulfur proteins (in Complex I) and then to Q. Electrons from succinate pass through a flavoprotein and several Fe-S centers (in Complex II) on the way to Q. Glycerol 3-phosphate donates electrons to a flavoprotein (glycerol 3-phosphate dehydrogenase) on the outer face of the inner mitochondrial membrane, from which they pass to Q. Acyl-CoA dehydrogenase (the first enzyme of β oxidation) transfers electrons to electron-transferring flavoprotein (ETF), from which they pass to Q via ETF:ubiquinone oxidoreductase.

exergonic transfer to ubiquinone of a hydride ion from NADH and a proton from the matrix, expressed by

$$NADH + H^+ + Q \longrightarrow NAD^+ + QH_2 \qquad (19–1)$$

and (2) the endergonic transfer of four protons from the matrix to the intermembrane space. Complex I is therefore a proton pump driven by the energy of electron transfer, and the reaction it catalyzes is **vectorial:** it moves protons in a specific direction from one location (the matrix, which becomes negatively charged with the departure of protons) to another (the intermembrane space, which becomes positively charged). To emphasize the vectorial nature of the process, the overall reaction is often written with subscripts that indicate the location of the protons: P for the positive side of the inner membrane (the intermembrane space), N for the negative side (the matrix):

$$NADH + 5H^+_N + Q \longrightarrow NAD^+ + QH_2 + 4H^+_P \qquad (19–2)$$

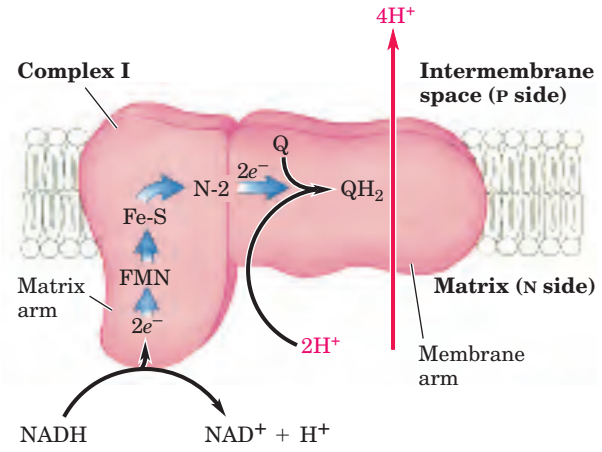

FIGURE 19–9 NADH:ubiquinone oxidoreductase (Complex I). Complex I catalyzes the transfer of a hydride ion from NADH to FMN, from which two electrons pass through a series of Fe-S centers to the iron-sulfur protein N-2 in the matrix arm of the complex. Electron transfer from N-2 to ubiquinone on the membrane arm forms QH_2, which diffuses into the lipid bilayer. This electron transfer also drives the expulsion from the matrix of four protons per pair of electrons. The detailed mechanism that couples electron and proton transfer in Complex I is not yet known, but probably involves a Q cycle similar to that in Complex III in which QH_2 participates twice per electron pair (see Fig. 19–12). Proton flux produces an electrochemical potential across the inner mitochondrial membrane (N side negative, P side positive), which conserves some of the energy released by the electron-transfer reactions. This electrochemical potential drives ATP synthesis.

Amytal (a barbiturate drug), rotenone (a plant product commonly used as an insecticide), and piericidin A (an antibiotic) inhibit electron flow from the Fe-S centers of Complex I to ubiquinone (Table 19–4) and therefore block the overall process of oxidative phosphorylation.

Ubiquinol (QH_2, the fully reduced form; Fig. 19–2) diffuses in the inner mitochondrial membrane from Complex I to Complex III, where it is oxidized to Q in a process that also involves the outward movement of H^+.

Complex II: Succinate to Ubiquinone We encountered **Complex II** in Chapter 16 as **succinate dehydrogenase,** the only membrane-bound enzyme in the citric acid cycle (p. 612). Although smaller and simpler than Complex I, it contains five prosthetic groups of two types and four different protein subunits (Fig. 19–10). Subunits C and D are integral membrane proteins, each with three transmembrane helices. They contain a heme group, heme *b,* and a binding site for ubiquinone, the final electron acceptor in the reaction catalyzed by Complex II. Subunits A and B extend into the matrix (or the cytosol of a bacterium); they contain three 2Fe-2S centers, bound FAD, and a binding site for the substrate, succinate. The path of electron transfer from the succinate-binding site to FAD, then through the Fe-S centers to the Q-binding site, is more than 40 Å long, but none of the individual electron-transfer distances exceeds about 11 Å—a reasonable distance for rapid electron transfer (Fig. 19–10).

TABLE 19–4 Agents That Interfere with Oxidative Phosphorylation or Photophosphorylation

Type of interference	*Compound**	*Target/mode of action*
Inhibition of electron transfer	Cyanide	Inhibit cytochrome oxidase
	Carbon monoxide	
	Antimycin A	Blocks electron transfer from cytochrome *b* to cytochrome c_1
	Myxothiazol	Prevent electron transfer from Fe-S center to ubiquinone
	Rotenone	
	Amytal	
	Piericidin A	
	DCMU	Competes with Q_B for binding site in PSII
Inhibition of ATP synthase	Aurovertin	Inhibits F_1
	Oligomycin	Inhibit F_o and CF_o
	Venturicidin	
	DCCD	Blocks proton flow through F_o and CF_o
Uncoupling of phosphorylation from electron transfer	FCCP	Hydrophobic proton carriers
	DNP	
	Valinomycin	K^+ ionophore
	Thermogenin	In brown fat, forms proton-conducting pores in inner mitochondrial membrane
Inhibition of ATP-ADP exchange	Atractyloside	Inhibits adenine nucleotide translocase

*DCMU is 3-(3,4-dichlorophenyl)-1,1-dimethylurea; DCCD, dicyclohexylcarbodiimide; FCCP, cyanide-*p*-trifluoromethoxyphenylhydrazone; DNP, 2,4-dinitrophenol.

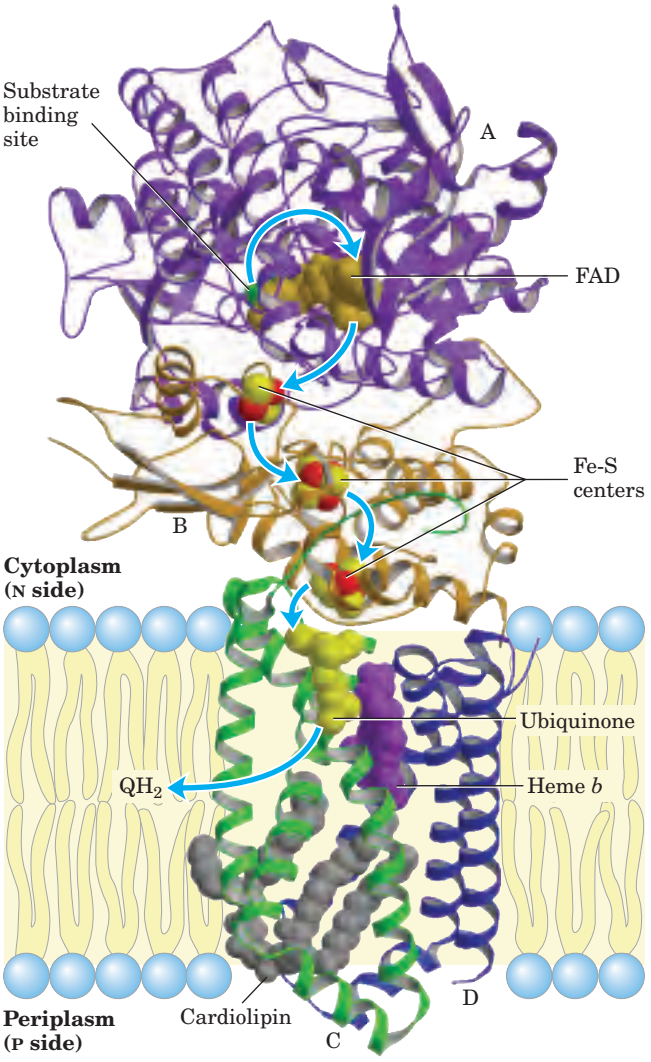

FIGURE 19–10 **Structure of Complex II (succinate dehydrogenase) of *E. coli*** (PDB ID 1NEK). The enzyme has two transmembrane subunits, C (green) and D (blue); the cytoplasmic extensions contain subunits B (orange) and A (purple). Just behind the FAD in subunit A (gold) is the binding site for succinate (occupied in this crystal structure by the inhibitor oxaloacetate, green). Subunit B has three sets of Fe-S centers (yellow and red); ubiquinone (yellow) is bound to subunit C; and heme *b* (purple) is sandwiched between subunits C and D. A cardiolipin molecule is so tightly bound to subunit C that it shows up in the crystal structure (gray spacefilling). Electrons move (blue arrows) from succinate to FAD, then through the three Fe-S centers to ubiquinone. The heme *b* is not on the main path of electron transfer but protects against the formation of reactive oxygen species (ROS) by electrons that go astray.

The heme *b* of Complex II is apparently not in the direct path of electron transfer; it may serve instead to reduce the frequency with which electrons "leak" out of the system, moving from succinate to molecular oxygen to produce the **reactive oxygen species (ROS)** hydrogen peroxide (H_2O_2) and the **superoxide radical** ($^{\cdot}O_2^-$) described in Section 19.5. Humans with point mutations in Complex II subunits near heme *b* or the quinone-binding site suffer from hereditary paraganglioma. This inherited condition is characterized by benign tumors of the head and neck, commonly in the carotid body, an organ that senses O_2 levels in the blood. These mutations result in greater production of ROS and perhaps greater tissue damage during succinate oxidation. ■

Other substrates for mitochondrial dehydrogenases pass electrons into the respiratory chain at the level of ubiquinone, but not through Complex II. The first step in the β oxidation of fatty acyl–CoA, catalyzed by the flavoprotein **acyl-CoA dehydrogenase** (see Fig. 17–8), involves transfer of electrons from the substrate to the FAD of the dehydrogenase, then to electron-transferring flavoprotein (ETF), which in turn passes its electrons to **ETF : ubiquinone oxidoreductase** (Fig. 19–8). This enzyme transfers electrons into the respiratory chain by reducing ubiquinone. Glycerol 3-phosphate, formed either from glycerol released by triacylglycerol breakdown or by the reduction of dihydroxyacetone phosphate from glycolysis, is oxidized by **glycerol 3-phosphate dehydrogenase** (see Fig. 17–4). This enzyme is a flavoprotein located on the outer face of the inner mitochondrial membrane, and like succinate dehydrogenase and acyl-CoA dehydrogenase it channels electrons into the respiratory chain by reducing ubiquinone (Fig. 19–8). The important role of glycerol 3-phosphate dehydrogenase in shuttling reducing equivalents from cytosolic NADH into the mitochondrial matrix is described in Section 19.2 (see Fig. 19–28). The effect of each of these electron-transferring enzymes is to contribute to the pool of reduced ubiquinone. QH_2 from all these reactions is reoxidized by Complex III.

Complex III: Ubiquinone to Cytochrome c The next respiratory complex, **Complex III,** also called **cytochrome bc_1 complex** or **ubiquinone:cytochrome *c* oxidoreductase,** couples the transfer of electrons from ubiquinol (QH_2) to cytochrome *c* with the vectorial transport of protons from the matrix to the intermembrane space. The determination of the complete structure of this huge complex (Fig. 19–11) and of Complex IV (below) by x-ray crystallography, achieved between 1995 and 1998, were landmarks in the study of mitochondrial electron transfer, providing the structural framework to integrate the many biochemical observations on the functions of the respiratory complexes.

Based on the structure of Complex III and detailed biochemical studies of the redox reactions, a reasonable model has been proposed for the passage of electrons

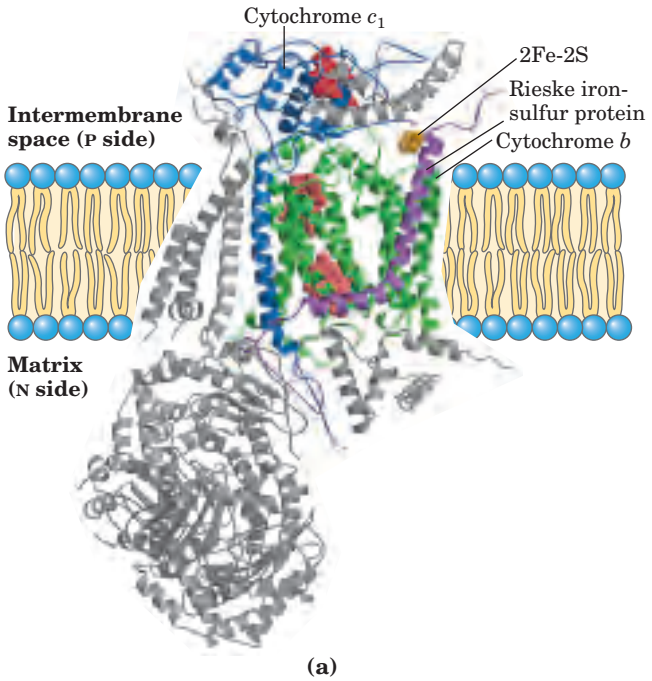

(a)

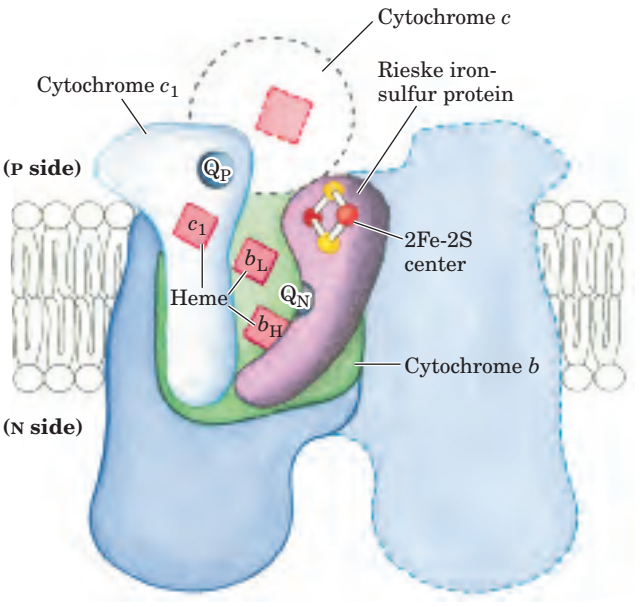

(b)

FIGURE 19–11 Cytochrome bc_1 complex (Complex III). The complex is a dimer of identical monomers, each with 11 different subunits. **(a)** Structure of a monomer. The functional core is three subunits: cytochrome b (green) with its two hemes (b_H and b_L, light red); the Rieske iron-sulfur protein (purple) with its 2Fe-2S centers (yellow); and cytochrome c_1 (blue) with its heme (red) (PDB ID 1BGY). **(b)** The dimeric functional unit. Cytochrome c_1 and the Rieske iron-sulfur protein project from the P surface and can interact with cytochrome c (not part of the functional complex) in the intermembrane space. The complex has two distinct binding sites for ubiquinone, Q_N and Q_P, which correspond to the sites of inhibition by two drugs that block oxidative phosphorylation. Antimycin A, which blocks electron flow from heme b_H to Q, binds at Q_N, close to heme b_H on the N (matrix) side of the membrane. Myxothiazol, which prevents electron flow from QH_2 to the Rieske iron-sulfur protein, binds at Q_P, near the 2Fe-2S center and heme b_L on the P side. The dimeric structure is essential to the function of Complex III. The interface between monomers forms two pockets, each containing a Q_P site from one monomer and a Q_N site from the other. The ubiquinone intermediates move within these sheltered pockets.

Complex III crystallizes in two distinct conformations (not shown). In one, the Rieske Fe-S center is close to its electron acceptor, the heme of cytochrome c_1, but relatively distant from cytochrome b and the QH_2-binding site at which the Rieske Fe-S center receives electrons. In the other, the Fe-S center has moved away from cytochrome c_1 and toward cytochrome b. The Rieske protein is thought to oscillate between these two conformations as it is reduced, then oxidized.

and protons through the complex. The net equation for the redox reactions of this **Q cycle** (Fig. 19–12) is

$$QH_2 + 2 \text{ cyt } c_1(\text{oxidized}) + 2H^+_N \longrightarrow Q + 2 \text{ cyt } c_1(\text{reduced}) + 4H^+_P \quad (19\text{–}3)$$

The Q cycle accommodates the switch between the two-electron carrier ubiquinone and the one-electron carriers—cytochromes b_{562}, b_{566}, c_1, and c—and explains the measured stoichiometry of four protons translocated per pair of electrons passing through the Complex III to cytochrome c. Although the path of electrons through this segment of the respiratory chain is complicated, the net effect of the transfer is simple: QH_2 is oxidized to Q and two molecules of cytochrome c are reduced.

Cytochrome c (see Fig. 4–18) is a soluble protein of the intermembrane space. After its single heme accepts an electron from Complex III, cytochrome c moves to Complex IV to donate the electron to a binuclear copper center.

Complex IV: Cytochrome c to O_2 In the final step of the respiratory chain, **Complex IV,** also called **cytochrome oxidase,** carries electrons from cytochrome c to molecular oxygen, reducing it to H_2O. Complex IV is a large enzyme (13 subunits; M_r 204,000) of the inner mitochondrial membrane. Bacteria contain a form that is much simpler, with only three or four subunits, but still capable of catalyzing both electron transfer and proton pumping. Comparison of the mitochondrial and bacterial complexes suggests that three subunits are critical to the function (Fig. 19–13).

Mitochondrial subunit II contains two Cu ions complexed with the —SH groups of two Cys residues in a binuclear center (Cu_A; Fig. 19–13b) that resembles the 2Fe-2S centers of iron-sulfur proteins. Subunit I contains two heme groups, designated a and a_3, and another copper ion (Cu_B). Heme a_3 and Cu_B form a second binuclear center that accepts electrons from heme a and transfers them to O_2 bound to heme a_3.

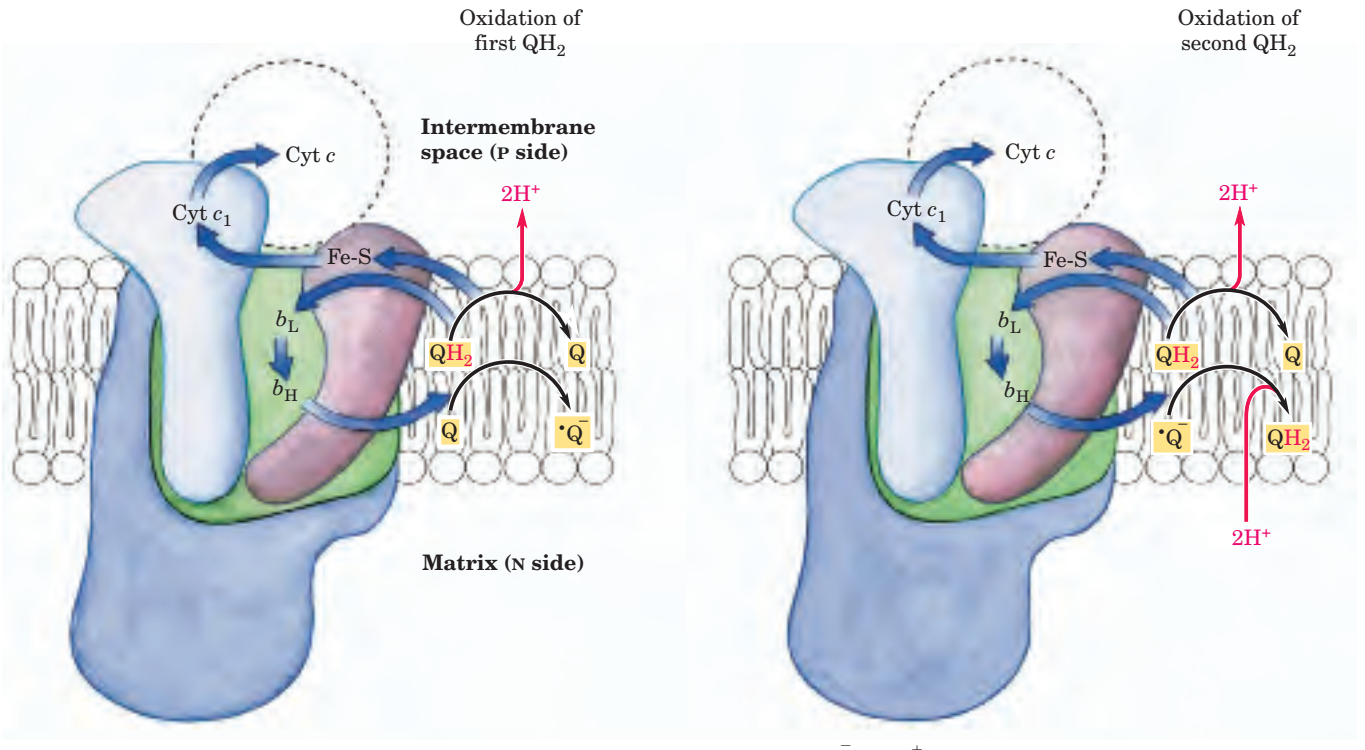

$$QH_2 + \text{cyt } c_1\,(\text{oxidized}) \longrightarrow {}^{\bullet}Q^- + 2H_P^+ + \text{cyt } c_1\,(\text{reduced})$$

$$QH_2 + {}^{\bullet}Q^- + 2H_N^+ + \text{cyt } c_1\,(\text{oxidized}) \longrightarrow QH_2 + 2H_P^+ + Q + \text{cyt } c_1\,(\text{reduced})$$

Net equation:

$$QH_2 + 2\ \text{cyt } c_1\,(\text{oxidized}) + 2H_N^+ \longrightarrow Q + 2\ \text{cyt } c_1\,(\text{reduced}) + 4H_P^+$$

FIGURE 19–12 The Q cycle. The path of electrons through Complex III is shown by blue arrows. On the P side of the membrane, two molecules of QH_2 are oxidized to Q near the P side, releasing two protons per Q (four protons in all) into the intermembrane space. Each QH_2 donates one electron (via the Rieske Fe-S center) to cytochrome c_1, and one electron (via cytochrome b) to a molecule of Q near the N side, reducing it in two steps to QH_2. This reduction also uses two protons per Q, which are taken up from the matrix.

Electron transfer through Complex IV is from cytochrome c to the Cu_A center, to heme a, to the heme a_3–Cu_B center, and finally to O_2 (Fig. 19–14). For every four electrons passing through this complex, the enzyme consumes four "substrate" H^+ from the matrix (N side) in converting O_2 to $2H_2O$. It also uses the energy of this redox reaction to pump one proton outward into the intermembrane space (P side) for each electron that passes through, adding to the electrochemical potential produced by redox-driven proton transport through Complexes I and III. The overall reaction catalyzed by Complex IV is

$$4\ \text{Cyt } c\ (\text{reduced}) + 8H_N^+ + O_2 \longrightarrow 4\ \text{cyt } c\ (\text{oxidized}) + 4H_P^+ + 2H_2O \quad (19\text{–}4)$$

This four-electron reduction of O_2 involves redox centers that carry only one electron at a time, and it must occur without the release of incompletely reduced intermediates such as hydrogen peroxide or hydroxyl free radicals—very reactive species that would damage cellular components. The intermediates remain tightly bound to the complex until completely converted to water.

The Energy of Electron Transfer Is Efficiently Conserved in a Proton Gradient

The transfer of two electrons from NADH through the respiratory chain to molecular oxygen can be written as

$$NADH + H^+ + \tfrac{1}{2}O_2 \longrightarrow NAD^+ + H_2O \quad (19\text{–}5)$$

This net reaction is highly exergonic. For the redox pair NAD^+/NADH, $E'°$ is -0.320 V, and for the pair O_2/H_2O, $E'°$ is 0.816 V. The $\Delta E'°$ for this reaction is therefore 1.14 V, and the standard free-energy change (see Eqn 13–6, p. 510) is

$$\begin{aligned}\Delta G'° &= -n\mathcal{F}\Delta E'° \\ &= -2(96.5\ \text{kJ/V}\cdot\text{mol})(1.14\ \text{V}) \\ &= -220\ \text{kJ/mol (of NADH)}\end{aligned} \quad (19\text{–}6)$$

This *standard* free-energy change is based on the assumption of equal concentrations (1 M) of NADH and

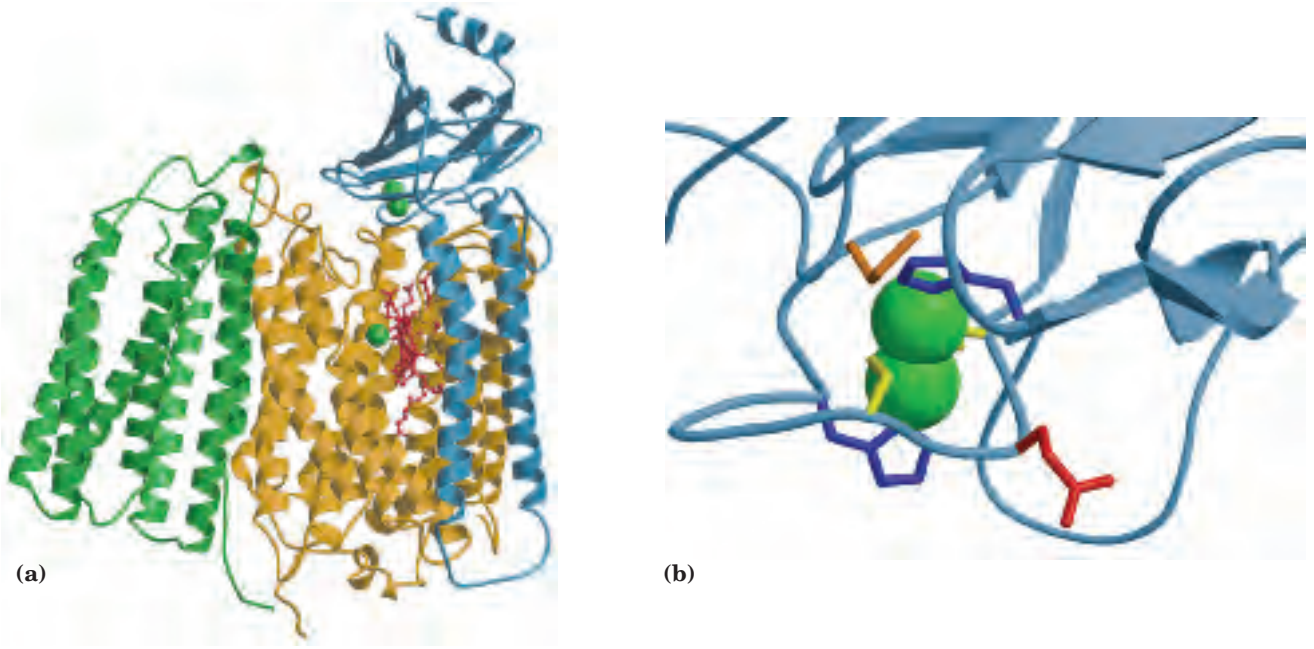

FIGURE 19–13 Critical subunits of cytochrome oxidase (Complex IV). The bovine complex is shown here (PDB ID 1OCC). **(a)** The core of Complex IV, with three subunits. Subunit I (yellow) has two heme groups, *a* and a_3 (red), and a copper ion, Cu_B (green sphere). Heme a_3 and Cu_B form a binuclear Fe-Cu center. Subunit II (blue) contains two Cu ions (green spheres) complexed with the —SH groups of two Cys residues in a binuclear center, Cu_A, that resembles the 2Fe-2S centers of iron-sulfur proteins. This binuclear center and the cytochrome *c*–binding site are located in a domain of subunit II that protrudes from the P side of the inner membrane (into the intermembrane space). Subunit III (green) seems to be essential for Complex IV function, but its role is not well understood. **(b)** The binuclear center of Cu_A. The Cu ions (green spheres) share electrons equally. When the center is reduced they have the formal charges $Cu^{1+}Cu^{1+}$; when oxidized, $Cu^{1.5+}Cu^{1.5+}$. Ligands around the Cu ions include two His (dark blue), two Cys (yellow), an Asp (red), and Met (orange) residues.

NAD$^+$. In actively respiring mitochondria, the actions of many dehydrogenases keep the actual [NADH]/[NAD$^+$] ratio well above unity, and the real free-energy change for the reaction shown in Equation 19–5 is therefore substantially greater (more negative) than −220 kJ/mol. A similar calculation for the oxidation of succinate shows that electron transfer from succinate ($E'°$ for fumarate/succinate = 0.031 V) to O_2 has a smaller, but still negative, standard free-energy change of about −150 kJ/mol.

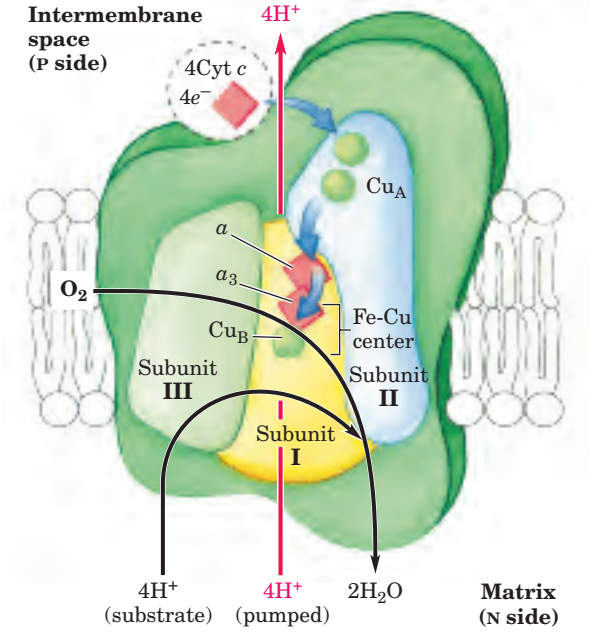

FIGURE 19–14 Path of electrons through Complex IV. The three proteins critical to electron flow are subunits I, II, and III. The larger green structure includes the other ten proteins in the complex. Electron transfer through Complex IV begins when two molecules of reduced cytochrome *c* (top) each donate an electron to the binuclear center Cu_A. From here electrons pass through heme *a* to the Fe-Cu center (cytochrome a_3 and Cu_B). Oxygen now binds to heme a_3 and is reduced to its peroxy derivative (O_2^{2-}) by two electrons from the Fe-Cu center. Delivery of two more electrons from cytochrome *c* (making four electrons in all) converts the O_2^{2-} to two molecules of water, with consumption of four "substrate" protons from the matrix. At the same time, four more protons are pumped from the matrix by an as yet unknown mechanism.

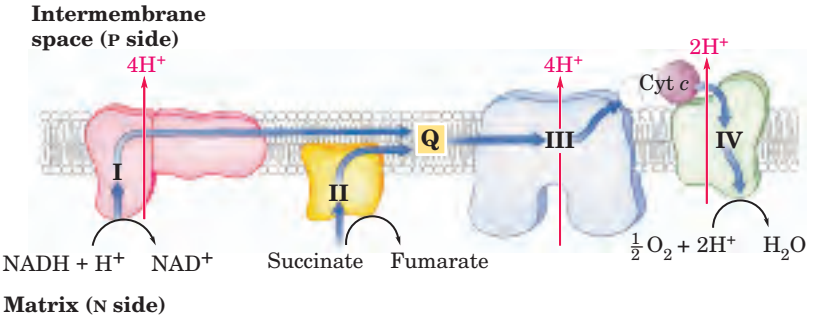

FIGURE 19–15 Summary of the flow of electrons and protons through the four complexes of the respiratory chain. Electrons reach Q through Complexes I and II. QH_2 serves as a mobile carrier of electrons and protons. It passes electrons to Complex III, which passes them to another mobile connecting link, cytochrome *c*. Complex IV then transfers electrons from reduced cytochrome *c* to O_2. Electron flow through Complexes I, III, and IV is accompanied by proton flow from the matrix to the intermembrane space. Recall that electrons from β oxidation of fatty acids can also enter the respiratory chain through Q (see Fig. 19–8).

Much of this energy is used to pump protons out of the matrix. For each pair of electrons transferred to O_2, four protons are pumped out by Complex I, four by Complex III, and two by Complex IV (Fig. 19–15). The *vectorial* equation for the process is therefore

$$NADH + 11H_N^+ + \tfrac{1}{2}O_2 \longrightarrow NAD^+ + 10H_P^+ + H_2O \qquad (19\text{–}7)$$

The electrochemical energy inherent in this difference in proton concentration and separation of charge represents a temporary conservation of much of the energy of electron transfer. The energy stored in such a gradient, termed the **proton-motive force,** has two components: (1) the *chemical potential energy* due to the difference in concentration of a chemical species (H^+) in the two regions separated by the membrane, and (2) the *electrical potential energy* that results from the separation of charge when a proton moves across the membrane without a counterion (Fig. 19–16).

As we showed in Chapter 11, the free-energy change for the creation of an electrochemical gradient by an ion pump is

$$\Delta G = RT \ln \left(\frac{C_2}{C_1}\right) + Z\mathcal{F}\Delta\psi \qquad (19\text{–}8)$$

where C_2 and C_1 are the concentrations of an ion in two regions, and $C_2 > C_1$; Z is the absolute value of its electrical charge (1 for a proton), and $\Delta\psi$ is the transmembrane difference in electrical potential, measured in volts.

For protons at 25 °C,

$$\ln \left(\frac{C_2}{C_1}\right) = 2.3(\log [H^+]_P - \log [H^+]_N)$$
$$= 2.3(pH_N - pH_P) = 2.3\ \Delta pH$$

and Equation 19–8 reduces to

$$\Delta G = 2.3RT\,\Delta pH + \mathcal{F}\Delta\psi \qquad (19\text{–}9)$$
$$= (5.70\ kJ/mol)\Delta pH + (96.5\ kJ/V \cdot mol)\Delta\psi$$

In actively respiring mitochondria, the measured $\Delta\psi$ is 0.15 to 0.20 V and the pH of the matrix is about 0.75 units more alkaline than that of the intermembrane space, so the calculated free-energy change for pumping protons outward is about 20 kJ/mol (of H^+), most of which is contributed by the electrical portion of the electrochemical potential. Because the transfer of two electrons from NADH to O_2 is accompanied by the outward pumping of 10 H^+ (Eqn 19–7), roughly 200 kJ of the 220 kJ released by oxidation of a mole of NADH is conserved in the proton gradient.

When protons flow spontaneously *down* their electrochemical gradient, energy is made available to do work. In mitochondria, chloroplasts, and aerobic bacteria, the electrochemical energy in the proton gradient drives the synthesis of ATP from ADP and P_i. We return to the energetics and stoichiometry of ATP synthesis driven by the electrochemical potential of the proton gradient in Section 19.2.

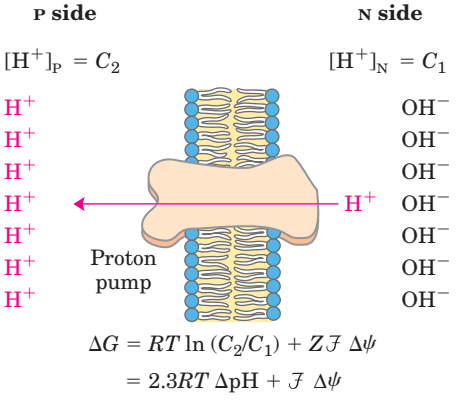

FIGURE 19–16 Proton-motive force. The inner mitochondrial membrane separates two compartments of different [H^+], resulting in differences in chemical concentration (ΔpH) and charge distribution ($\Delta\psi$) across the membrane. The net effect is the proton-motive force (ΔG), which can be calculated as shown here. This is explained more fully in the text.

Plant Mitochondria Have Alternative Mechanisms for Oxidizing NADH

Plant mitochondria supply the cell with ATP during periods of low illumination or darkness by mechanisms entirely analogous to those used by nonphotosynthetic organisms. In the light, the principal source of mitochondrial NADH is a reaction in which glycine, produced by a process known as photorespiration, is converted to serine (see Fig. 20–21):

$$2\ \text{Glycine} + \text{NAD}^+ \longrightarrow \text{serine} + \text{CO}_2 + \text{NH}_3 + \text{NADH} + \text{H}^+$$

For reasons discussed in Chapter 20, plants must carry out this reaction even when they do not need NADH for ATP production. To regenerate NAD^+ from unneeded NADH, plant mitochondria transfer electrons from NADH directly to ubiquinone and from ubiquinone directly to O_2, bypassing Complexes III and IV and their proton pumps. In this process the energy in NADH is dissipated as heat, which can sometimes be of value to the plant (Box 19–1). Unlike cytochrome oxidase (Complex IV), the alternative QH_2 oxidase is not inhibited by cyanide. Cyanide-resistant NADH oxidation is therefore the hallmark of this unique plant electron-transfer pathway.

SUMMARY 19.1 Electron-Transfer Reactions in Mitochondria

- Chemiosmotic theory provides the intellectual framework for understanding many biological energy transductions, including oxidative phosphorylation and photophosphorylation. The mechanism of energy coupling is similar in both cases: the energy of electron flow is conserved by the concomitant pumping of protons across the membrane, producing an electrochemical gradient, the proton-motive force.
- In mitochondria, hydride ions removed from substrates by NAD-linked dehydrogenases donate electrons to the respiratory (electron-transfer) chain, which transfers the electrons to molecular O_2, reducing it to H_2O.
- Shuttle systems convey reducing equivalents from cytosolic NADH to mitochondrial NADH. Reducing equivalents from all NAD-linked dehydrogenations are transferred to mitochondrial NADH dehydrogenase (Complex I).
- Reducing equivalents are then passed through a series of Fe-S centers to ubiquinone, which transfers the electrons to cytochrome *b*, the first carrier in Complex III. In this complex, electrons take two separate paths through two *b*-type cytochromes and cytochrome c_1 to an Fe-S center. The Fe-S center passes electrons, one at a time, through cytochrome *c* and into Complex IV, cytochrome oxidase. This copper-containing enzyme, which also contains cytochromes *a* and a_3, accumulates electrons, then passes them to O_2, reducing it to H_2O.
- Some electrons enter this chain of carriers through alternative paths. Succinate is oxidized by succinate dehydrogenase (Complex II), which contains a flavoprotein that passes electrons through several Fe-S centers to ubiquinone. Electrons derived from the oxidation of fatty acids pass to ubiquinone via the electron-transferring flavoprotein.
- Plants also have an alternative, cyanide-resistant NADH oxidation pathway.

19.2 ATP Synthesis

How is a concentration gradient of protons transformed into ATP? We have seen that electron transfer releases, and the proton-motive force conserves, more than enough free energy (about 200 kJ) per "mole" of electron pairs to drive the formation of a mole of ATP, which requires about 50 kJ (see Box 13–1). Mitochondrial oxidative phosphorylation therefore poses no thermodynamic problem. But what is the chemical mechanism that couples proton flux with phosphorylation?

Peter Mitchell, 1920–1992

The **chemiosmotic model,** proposed by Peter Mitchell, is the paradigm for this mechanism. According to the model (Fig. 19–17), the electrochemical energy inherent in the difference in proton concentration and separation of charge across the inner mitochondrial membrane—the proton-motive force—drives the synthesis of ATP as protons flow passively back into the matrix through a proton pore associated with **ATP synthase.** To emphasize this crucial role of the proton-motive force, the equation for ATP synthesis is sometimes written

$$\text{ADP} + \text{P}_\text{i} + n\text{H}^+_\text{P} \longrightarrow \text{ATP} + \text{H}_2\text{O} + n\text{H}^+_\text{N} \qquad (19\text{–}10)$$

Mitchell used "chemiosmotic" to describe enzymatic reactions that involve, simultaneously, a chemical reaction and a transport process. The operational definition of "coupling" is shown in Figure 19–18. When isolated mitochondria are suspended in a buffer containing ADP, P_i, and an oxidizable substrate such as succinate, three easily measured processes occur: (1) the substrate is oxidized (succinate yields fumarate), (2) O_2 is consumed, and (3) ATP is synthesized. Oxygen consumption and ATP synthesis depend on the presence of an oxidizable substrate (succinate in this case) as well as ADP and P_i.

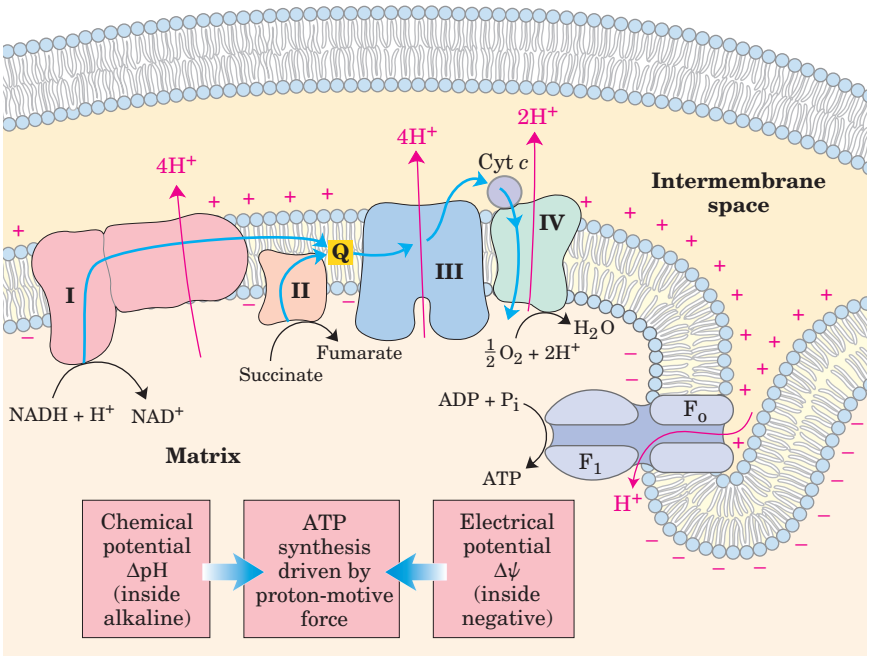

FIGURE 19–17 Chemiosmotic model. In this simple representation of the chemiosmotic theory applied to mitochondria, electrons from NADH and other oxidizable substrates pass through a chain of carriers arranged asymmetrically in the inner membrane. Electron flow is accompanied by proton transfer across the membrane, producing both a chemical gradient (ΔpH) and an electrical gradient ($\Delta\psi$). The inner mitochondrial membrane is impermeable to protons; protons can reenter the matrix only through proton-specific channels (F_o). The proton-motive force that drives protons back into the matrix provides the energy for ATP synthesis, catalyzed by the F_1 complex associated with F_o.

Because the energy of substrate oxidation drives ATP synthesis in mitochondria, we would expect inhibitors of the passage of electrons to O_2 (such as cyanide, carbon monoxide, and antimycin A) to block ATP synthesis (Fig. 19–18a). More surprising is the finding that the converse is also true: inhibition of ATP synthesis blocks electron transfer in intact mitochondria. This obligatory coupling can be demonstrated in isolated mitochondria by providing O_2 and oxidizable substrates, but not ADP (Fig. 19–18b). Under these conditions, no ATP synthesis can occur and electron transfer to O_2 does not proceed. Coupling of oxidation and phosphorylation can also be demonstrated using oligomycin or venturicidin, toxic antibiotics that bind to the ATP synthase in mitochondria. These compounds are potent inhibitors of both ATP synthesis *and* the transfer of electrons through the chain of carriers to O_2 (Fig. 19–18b). Because oligomycin is known to interact not directly with the electron carriers but with ATP synthase, it follows that electron transfer and ATP synthesis are obligately coupled; neither reaction occurs without the other.

Chemiosmotic theory readily explains the dependence of electron transfer on ATP synthesis in mitochondria. When the flow of protons into the matrix through the proton channel of ATP synthase is blocked (with oligomycin, for example), no path exists for the return of protons to the matrix, and the continued extrusion of protons driven by the activity of the respiratory chain generates a large proton gradient. The proton-motive force builds up until the cost (free energy) of pumping

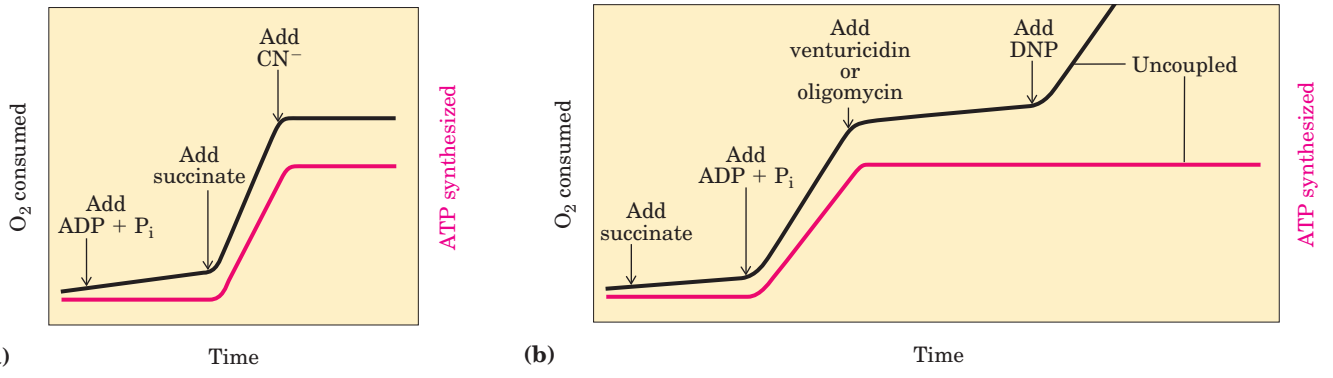

FIGURE 19–18 Coupling of electron transfer and ATP synthesis in mitochondria. In experiments to demonstrate coupling, mitochondria are suspended in a buffered medium and an O_2 electrode monitors O_2 consumption. At intervals, samples are removed and assayed for the presence of ATP. **(a)** Addition of ADP and P_i alone results in little or no increase in either respiration (O_2 consumption; black) or ATP synthesis (red). When succinate is added, respiration begins immediately and ATP is synthesized. Addition of cyanide (CN^-), which blocks electron transfer between cytochrome oxidase and O_2, inhibits both respiration and ATP synthesis. **(b)** Mitochondria provided with succinate respire and synthesize ATP only when ADP and P_i are added. Subsequent addition of venturicidin or oligomycin, inhibitors of ATP synthase, blocks both ATP synthesis and respiration. Dinitrophenol (DNP) is an uncoupler, allowing respiration to continue without ATP synthesis.

BOX 19–1 THE WORLD OF BIOCHEMISTRY

Hot, Stinking Plants and Alternative Respiratory Pathways

Many flowering plants attract insect pollinators by releasing odorant molecules that mimic an insect's natural food sources or potential egg-laying sites. Plants pollinated by flies or beetles that normally feed on or lay their eggs in dung or carrion sometimes use foul-smelling compounds to attract these insects.

One family of stinking plants is the Araceae, which includes philodendrons, arum lilies, and skunk cabbages. These plants have tiny flowers densely packed on an erect structure, the spadix, surrounded by a modified leaf, the spathe. The spadix releases odors of rotting flesh or dung. Before pollination the spadix also heats up, in some species to as much as 20 to 40 °C above the ambient temperature. Heat production (thermogenesis) helps evaporate odorant molecules for better dispersal, and because rotting flesh and dung are usually warm from the hyperactive metabolism of scavenging microbes, the heat itself might also attract insects. In the case of the eastern skunk cabbage (Fig. 1), which flowers in late winter or early spring when snow still covers the ground, thermogenesis allows the spadix to grow up through the snow.

How does a skunk cabbage heat its spadix? The mitochondria of plants, fungi, and unicellular eukaryotes have electron-transfer systems that are essentially the same as those in animals, but they also have an alternative respiratory pathway. A cyanide-resistant QH_2 oxidase transfers electrons from the ubiquinone pool directly to oxygen, bypassing the two proton-translocating steps of Complexes III and IV (Fig. 2). Energy that might have been conserved as ATP is instead released as heat. Plant mitochondria also have an alternative NADH dehydrogenase, insensitive to the Complex I inhibitor rotenone (see Table 19–4), that transfers electrons from NADH in the matrix directly to ubiquinone, bypassing Complex I and its associated proton pumping. And plant mitochondria have yet another NADH dehydrogenase, on the external face of the inner membrane, that transfers electrons from NADPH or NADH in the intermembrane space to ubiquinone, again bypassing Complex I. Thus when electrons enter the alternative respiratory pathway through the rotenone-insensitive NADH dehydrogenase, the external NADH dehydrogenase, or succinate dehydrogenase (Complex II), and pass to O_2 via the cyanide-resistant alternative oxidase, energy is not conserved as ATP but is released as heat. A skunk cabbage can use the heat to melt snow, produce a foul stench, or attract beetles or flies.

FIGURE 1 Eastern skunk cabbage.

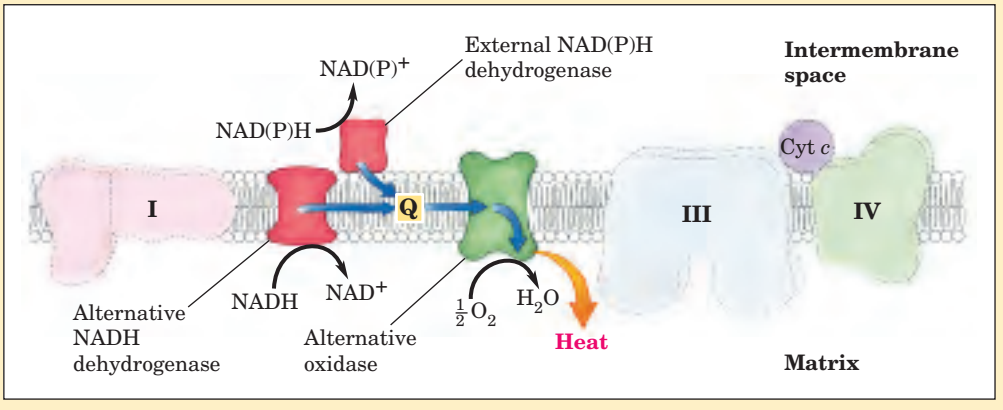

FIGURE 2 Electron carriers of the inner membrane of plant mitochondria. Electrons can flow through Complexes I, III, and IV, as in animal mitochondria, or through plant-specific alternative carriers by the paths shown with blue arrows.

protons out of the matrix against this gradient equals or exceeds the energy released by the transfer of electrons from NADH to O_2. At this point electron flow must stop; the free energy for the overall process of electron flow coupled to proton pumping becomes zero, and the system is at equilibrium.

Certain conditions and reagents, however, can uncouple oxidation from phosphorylation. When intact mitochondria are disrupted by treatment with detergent or by physical shear, the resulting membrane fragments can still catalyze electron transfer from succinate or NADH to O_2, but no ATP synthesis is coupled to this respiration. Certain chemical compounds cause uncoupling without disrupting mitochondrial structure. Chemical uncouplers include 2,4-dinitrophenol (DNP) and carbonylcyanide-*p*-trifluoromethoxyphenylhydrazone (FCCP) (Table 19–4; Fig. 19–19), weak acids with hydrophobic properties that permit them to diffuse readily across mitochondrial membranes. After entering the matrix in the protonated form, they can release a proton, thus dissipating the proton gradient. Ionophores such as valinomycin (see Fig. 11–45) allow inorganic ions to pass easily through membranes. Ionophores uncouple electron transfer from oxidative phosphorylation by dissipating the electrical contribution to the electrochemical gradient across the mitochondrial membrane.

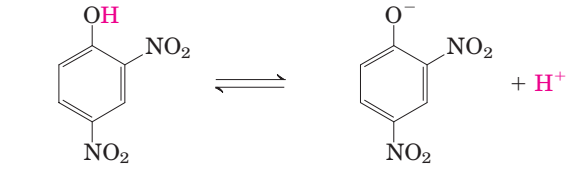

2,4-Dinitrophenol (DNP)

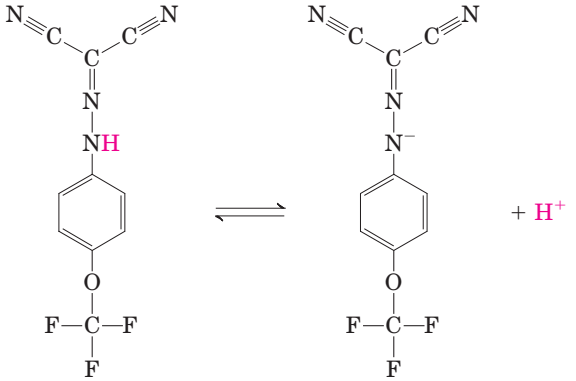

Carbonylcyanide-*p*-trifluoromethoxyphenylhydrazone (FCCP)

FIGURE 19–19 **Two chemical uncouplers of oxidative phosphorylation.** Both DNP and FCCP have a dissociable proton and are very hydrophobic. They carry protons across the inner mitochondrial membrane, dissipating the proton gradient. Both also uncouple photophosphorylation (see Fig. 19–57).

A prediction of the chemiosmotic theory is that, because the role of electron transfer in mitochondrial ATP synthesis is simply to pump protons to create the electrochemical potential of the proton-motive force, an artificially created proton gradient should be able to replace electron transfer in driving ATP synthesis. This has been experimentally confirmed (Fig. 19–20). Mitochondria manipulated so as to impose a difference of proton concentration and a separation of charge across the inner membrane synthesize ATP *in the absence of an oxidizable substrate;* the proton-motive force alone suffices to drive ATP synthesis.

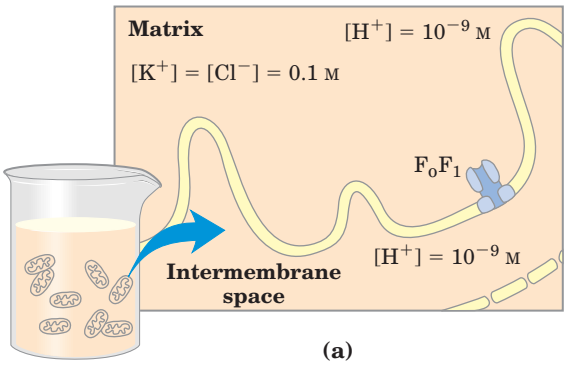

(a)

pH lowered from 9 to 7; valinomycin present; no K^+

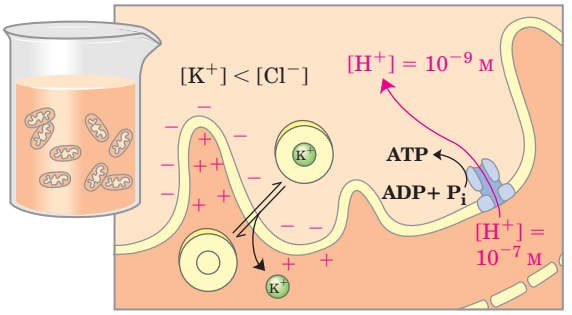

(b)

FIGURE 19–20 **Evidence for the role of a proton gradient in ATP synthesis.** An artificially imposed electrochemical gradient can drive ATP synthesis in the absence of an oxidizable substrate as electron donor. In this two-step experiment, **(a)** isolated mitochondria are first incubated in a pH 9 buffer containing 0.1 M KCl. Slow leakage of buffer and KCl into the mitochondria eventually brings the matrix into equilibrium with the surrounding medium. No oxidizable substrates are present. **(b)** Mitochondria are now separated from the pH 9 buffer and resuspended in pH 7 buffer containing valinomycin but no KCl. The change in buffer creates a difference of two pH units across the inner mitochondrial membrane. The outward flow of K^+, carried (by valinomycin) down its concentration gradient without a counterion, creates a charge imbalance across the membrane (matrix negative). The sum of the chemical potential provided by the pH difference and the electrical potential provided by the separation of charges is a proton-motive force large enough to support ATP synthesis in the absence of an oxidizable substrate.

ATP Synthase Has Two Functional Domains, F_o and F_1

Mitochondrial **ATP synthase** is an F-type ATPase (see Fig. 11–39; Table 11–3) similar in structure and mechanism to the ATP synthases of chloroplasts and eubacteria. This large enzyme complex of the inner mitochondrial membrane catalyzes the formation of ATP from ADP and P_i, accompanied by the flow of protons from the P to the N side of the membrane (Eqn 19–10). ATP synthase, also called Complex V, has two distinct components: F_1, a peripheral membrane protein, and F_o (*o* denoting oligomycin-sensitive), which is integral to the membrane. F_1, the first factor recognized as essential for oxidative phosphorylation, was identified and purified by Efraim Racker and his colleagues in the early 1960s.

Efraim Racker, 1913–1991

In the laboratory, small membrane vesicles formed from inner mitochondrial membranes carry out ATP synthesis coupled to electron transfer. When F_1 is gently extracted, the "stripped" vesicles still contain intact respiratory chains and the F_o portion of ATP synthase. The vesicles can catalyze electron transfer from NADH to O_2 but cannot produce a proton gradient: F_o has a proton pore through which protons leak as fast as they are pumped by electron transfer, and without a proton gradient the F_1-depleted vesicles cannot make ATP. Isolated F_1 catalyzes ATP hydrolysis (the reversal of synthesis) and was therefore originally called **F_1ATPase.** When purified F_1 is added back to the depleted vesicles, it reassociates with F_o, plugging its proton pore and restoring the membrane's capacity to couple electron transfer and ATP synthesis.

ATP Is Stabilized Relative to ADP on the Surface of F_1

Isotope exchange experiments with purified F_1 reveal a remarkable fact about the enzyme's catalytic mechanism: on the enzyme surface, the reaction ADP + P_i $\rightleftharpoons$ ATP + H_2O is readily reversible—the free-energy change for ATP synthesis is close to zero! When ATP is hydrolyzed by F_1 in the presence of ^{18}O-labeled water, the P_i released contains an ^{18}O atom. Careful measurement of the ^{18}O content of P_i formed in vitro by F_1-catalyzed hydrolysis of ATP reveals that the P_i has not one, but three or four ^{18}O atoms (Fig. 19–21). This indicates that the terminal pyrophosphate bond in ATP is cleaved and re-formed repeatedly before P_i leaves the enzyme surface. With P_i free to tumble in its binding site, each hydrolysis inserts ^{18}O randomly at one of the

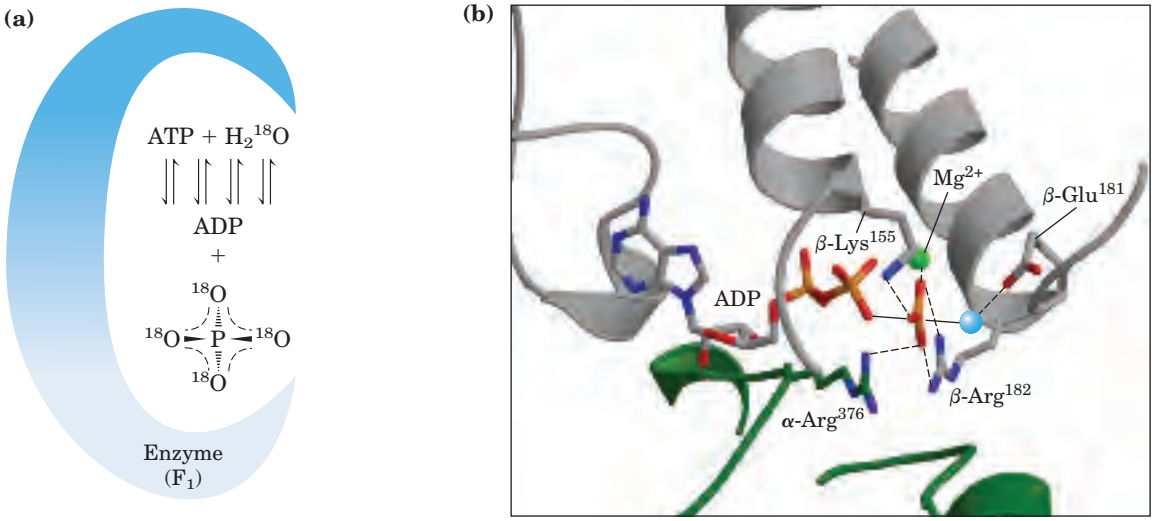

FIGURE 19–21 Catalytic mechanism of F_1. (a) ^{18}O-exchange experiment. F_1 solubilized from mitochondrial membranes is incubated with ATP in the presence of ^{18}O-labeled water. At intervals, a sample of the solution is withdrawn and analyzed for the incorporation of ^{18}O into the P_i produced from ATP hydrolysis. In minutes, the P_i contains three or four ^{18}O atoms, indicating that both ATP hydrolysis and ATP synthesis have occurred several times during the incubation. **(b)** The likely transition state complex for ATP hydrolysis and synthesis in ATP synthase (derived from PDB ID 1BMF). The α subunit is shown in green, β in gray. The positively charged residues β-Arg^{182} and α-Arg^{376} coordinate two oxygens of the pentavalent phosphate intermediate; β-Lys^{155} interacts with a third oxygen, and the Mg^{2+} ion (green sphere) further stabilizes the intermediate. The blue sphere represents the leaving group (H_2O). These interactions result in the ready equilibration of ATP and ADP + P_i in the active site.

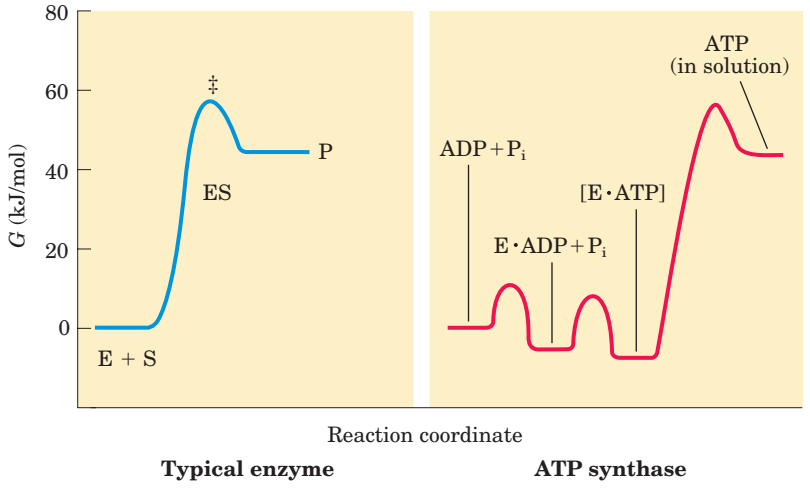

FIGURE 19–22 Reaction coordinate diagrams for ATP synthase and for a more typical enzyme. In a typical enzyme-catalyzed reaction (left), reaching the transition state (‡) between substrate and product is the major energy barrier to overcome. In the reaction catalyzed by ATP synthase (right), release of ATP from the enzyme, not formation of ATP, is the major energy barrier. The free-energy change for the formation of ATP from ADP and P_i in aqueous solution is large and positive, but on the enzyme surface, the very tight binding of ATP provides sufficient binding energy to bring the free energy of the enzyme-bound ATP close to that of ADP + P_i, so the reaction is readily reversible. The equilibrium constant is near 1. The free energy required for the release of ATP is provided by the proton-motive force.

four positions in the molecule. This exchange reaction occurs in unenergized F_oF_1 complexes (with no proton gradient) and with isolated F_1—the exchange does not require the input of energy.

Kinetic studies of the initial rates of ATP synthesis and hydrolysis confirm the conclusion that $\Delta G'^\circ$ for ATP synthesis on the enzyme is near zero. From the measured rates of hydrolysis ($k_1 = 10\ s^{-1}$) and synthesis ($k_{-1} = 24\ s^{-1}$), the calculated equilibrium constant for the reaction

$$\text{Enz-ATP} \rightleftharpoons \text{Enz–(ADP + } P_i\text{)}$$

is

$$K'_{eq} = \frac{k_{-1}}{k_1} = \frac{24\ s^{-1}}{10\ s^{-1}} = 2.4$$

From this K'_{eq}, the calculated apparent $\Delta G'^\circ$ is close to zero. This is much different from the K'_{eq} of about 10^5 ($\Delta G'^\circ = -30.5$ kJ/mol) for the hydrolysis of ATP free in solution (not on the enzyme surface).

What accounts for the huge difference? ATP synthase stabilizes ATP relative to ADP + P_i by binding ATP more tightly, releasing enough energy to counterbalance the cost of making ATP. Careful measurements of the binding constants show that F_oF_1 binds ATP with very high affinity ($K_d \leq 10^{-12}$ M) and ADP with much lower affinity ($K_d \approx 10^{-5}$ M). The difference in K_d corresponds to a difference of about 40 kJ/mol in binding energy, and this binding energy drives the equilibrium toward formation of the product ATP.

The Proton Gradient Drives the Release of ATP from the Enzyme Surface

Although ATP synthase equilibrates ATP with ADP + P_i, in the absence of a proton gradient the newly synthesized ATP does not leave the surface of the enzyme. It is the proton gradient that causes the enzyme to release the ATP formed on its surface. The reaction coordinate diagram of the process (Fig. 19–22) illustrates the difference between the mechanism of ATP synthase and that of many other enzymes that catalyze endergonic reactions.

For the continued synthesis of ATP, the enzyme must cycle between a form that binds ATP very tightly and a form that releases ATP. Chemical and crystallographic studies of the ATP synthase have revealed the structural basis for this alternation in function.

Each β Subunit of ATP Synthase Can Assume Three Different Conformations

Mitochondrial F_1 has nine subunits of five different types, with the composition $\alpha_3\beta_3\gamma\delta\varepsilon$. Each of the three β subunits has one catalytic site for ATP synthesis. The crystallographic determination of the F_1 structure by John E. Walker and colleagues revealed structural details very helpful in explaining the catalytic mechanism of the enzyme. The knoblike portion of F_1 is a flattened sphere, 8 nm high and 10 nm across, consisting of alternating α and β subunits arranged like the sections of an orange (Fig. 19–23a–c). The polypeptides that make up the stalk in the F_1 crystal structure are asymmetrically arranged, with one domain of the single γ subunit making up a central shaft that passes through F_1, and another domain of γ associated primarily with one of the three β subunits, designated β-empty (Fig. 19–23c). Although the amino acid sequences of the three β subunits are identical, *their conformations differ,* in part because of the association of the γ subunit with just one of the three. The structures of the δ and ε subunits are not revealed in these crystallographic studies.

The conformational differences among β subunits extend to differences in their ATP/ADP-binding sites.

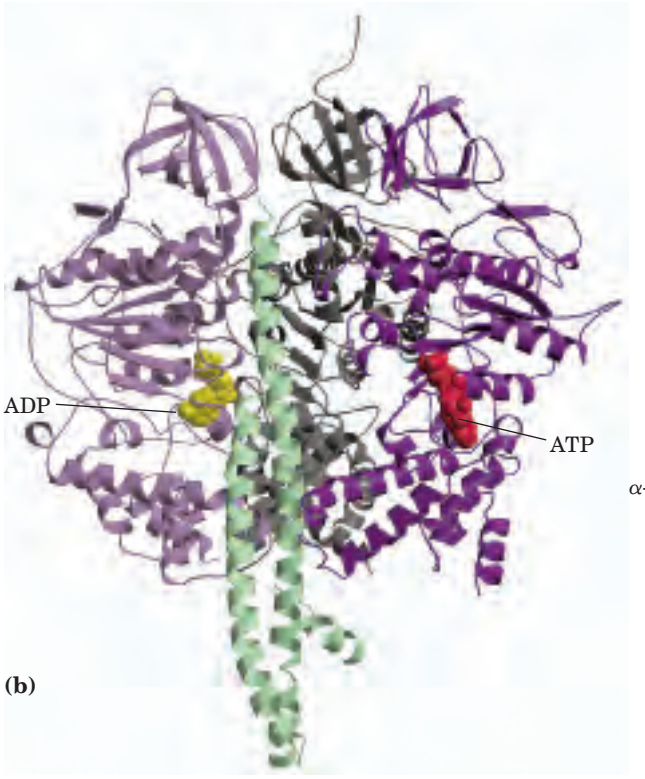

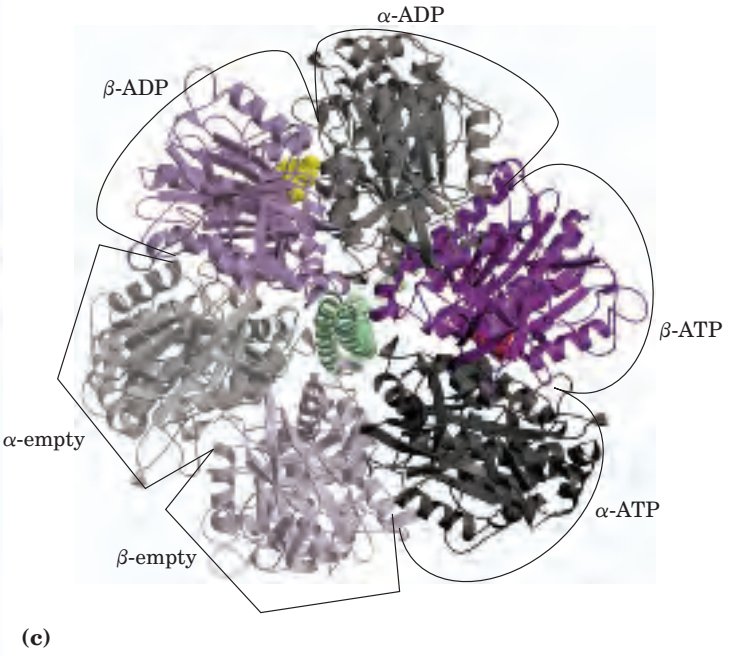

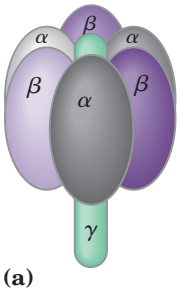

John E. Walker

FIGURE 19–23 Mitochondrial ATP synthase complex. (a) Structure of the F_1 complex, deduced from crystallographic and biochemical studies. In F_1, three α and three β subunits are arranged like the segments of an orange, with alternating α (shades of gray) and β (shades of purple) subunits around a central shaft, the γ subunit (green). **(b)** Crystal structure of bovine F_1 (PDB ID 1BMF), viewed from the side. Two α subunits and one β subunit have been omitted to reveal the central shaft (γ subunit) and the binding sites for ATP (red) and ADP (yellow) on the β subunits. The δ and ε subunits are not shown here. **(c)** F_1 viewed from above (that is, from the N side of the membrane), showing the three β and three α subunits and the central shaft (γ subunit, green). Each β subunit, near its interface with the neighboring α subunit, has a nucleotide-binding site critical to the catalytic activity. The single γ subunit associates primarily with one of the three $\alpha\beta$ pairs, forcing each of the three β subunits into slightly different conformations, with different nucleotide-binding sites. In the crystalline enzyme, one subunit (β-ADP) has ADP (yellow) in its binding site, the next (β-ATP) has ATP (red), and the third (β-empty) has no bound nucleotide. **(d)** Side view of the F_oF_1 structure. This is a composite, in which the crystallographic coordinates of bovine mitochondrial F_1 (shades of purple and gray) have been combined with those of yeast mitochondrial F_o (shades of yellow and orange) (PDB ID 1QO1). Subunits a, b, δ, and ε were not part of the crystal structure shown here. **(e)** The F_oF_1 structure, viewed end-on in the direction P side to N side. The major structures visible in this cross section are the two transmembrane helices of each of ten c subunits arranged in concentric circles. **(f)** Diagram of the F_oF_1 complex, deduced from biochemical and crystallographic studies. The two b subunits of F_o associate firmly with the α and β subunits of F_1, holding them fixed relative to the membrane. In F_o, the membrane-embedded cylinder of c subunits is attached to the shaft made up of F_1 subunits γ and ε. As protons flow through the membrane from the P side to the N side through F_o, the cylinder and shaft rotate, and the β subunits of F_1 change conformation as the γ subunit associates with each in turn.

When researchers crystallized the protein in the presence of ADP and App(NH)p, a close structural analog of ATP that cannot be hydrolyzed by the ATPase activity of F_1, the binding site of one of the three β subunits was filled with App(NH)p, the second was filled with

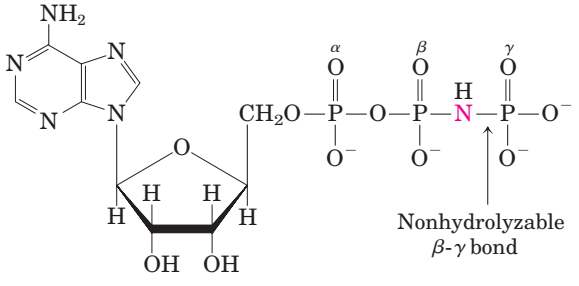

App(NH)p (β,γ-imidoadenosine 5′-triphosphate)

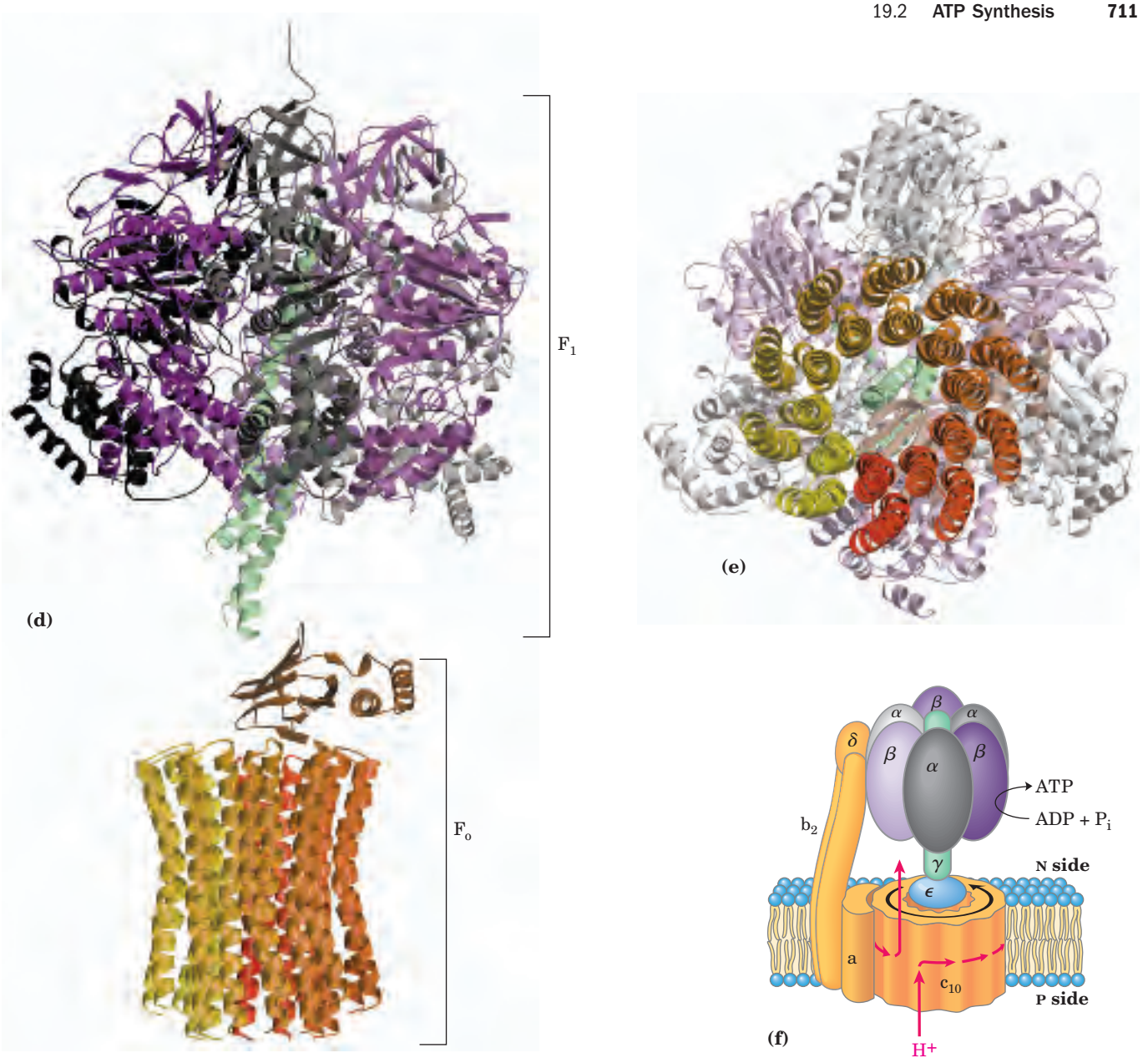

ADP, and the third was empty. The corresponding β subunit conformations are designated β-ATP, β-ADP, and β-empty (Fig. 19–23c). This difference in nucleotide binding among the three subunits is critical to the mechanism of the complex.

The F_o complex making up the proton pore is composed of three subunits, a, b, and c, in the proportion ab_2c_{10-12}. Subunit c is a small (M_r 8,000), very hydrophobic polypeptide, consisting almost entirely of two transmembrane helices, with a small loop extending from the matrix side of the membrane. The crystal structure of the yeast F_oF_1, solved in 1999, shows the arrangement of the c subunits. The yeast complex has ten c subunits, each with two transmembrane helices roughly perpendicular to the plane of the membrane and arranged in two concentric circles (Fig. 19–23d, e). The inner circle is made up of the amino-terminal helices of each c subunit; the outer circle, about 55 Å in diameter, is made up of the carboxyl-terminal helices. The ε and γ subunits of F_1 form a leg-and-foot that projects from the bottom (membrane) side of F_1 and stands firmly on the ring of c subunits. The schematic drawing in Figure 19–23f combines the structural information from studies of bovine F_1 and yeast F_oF_1.

Rotational Catalysis Is Key to the Binding-Change Mechanism for ATP Synthesis

On the basis of detailed kinetic and binding studies of the reactions catalyzed by F_oF_1, Paul Boyer proposed a **rotational catalysis** mechanism in which the three active sites of F_1 take turns catalyzing ATP synthesis

Paul Boyer

(Fig. 19–24). A given β subunit starts in the β-ADP conformation, which binds ADP and P_i from the surrounding medium. The subunit now changes conformation, assuming the β-ATP form that tightly binds and stabilizes ATP, bringing about the ready equilibration of ADP + P_i with ATP on the enzyme surface. Finally, the subunit changes to the β-empty conformation, which has very low affinity for ATP, and the newly synthesized ATP leaves the enzyme surface. Another round of catalysis begins when this subunit again assumes the β-ADP form and binds ADP and P_i.

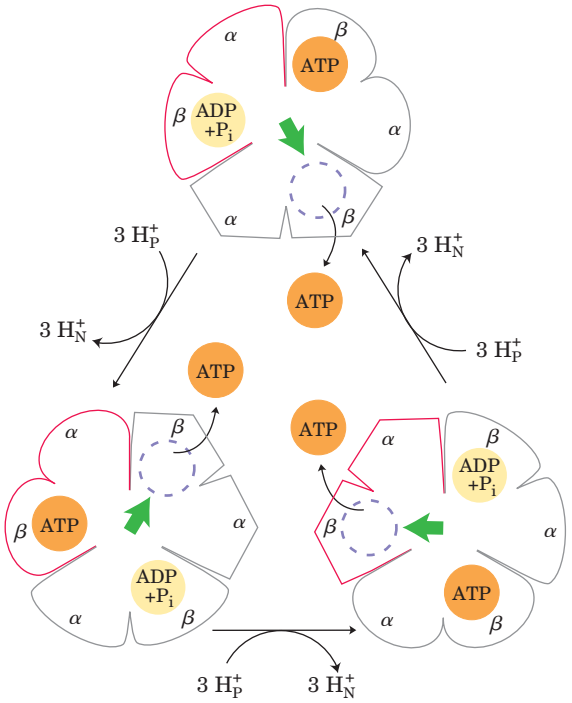

FIGURE 19–24 Binding-change model for ATP synthase. The F_1 complex has three nonequivalent adenine nucleotide–binding sites, one for each pair of α and β subunits. At any given moment, one of these sites is in the β-ATP conformation (which binds ATP tightly), a second is in the β-ADP (loose-binding) conformation, and a third is in the β-empty (very-loose-binding) conformation. The proton-motive force causes rotation of the central shaft—the γ subunit, shown as a green arrowhead—which comes into contact with each αβ subunit pair in succession. This produces a cooperative conformational change in which the β-ATP site is converted to the β-empty conformation, and ATP dissociates; the β-ADP site is converted to the β-ATP conformation, which promotes condensation of bound ADP + P_i to form ATP; and the β-empty site becomes a β-ADP site, which loosely binds ADP + P_i entering from the solvent. This model, based on experimental findings, requires that at least two of the three catalytic sites alternate in activity; ATP cannot be released from one site unless and until ADP and P_i are bound at the other.

The conformational changes central to this mechanism are driven by the passage of protons through the F_o portion of ATP synthase. The streaming of protons through the F_o "pore" causes the cylinder of c subunits and the attached γ subunit to rotate about the long axis of γ, which is perpendicular to the plane of the membrane. The γ subunit passes through the center of the $\alpha_3\beta_3$ spheroid, which is held stationary relative to the membrane surface by the b_2 and δ subunits (Fig. 19–23f). With each rotation of 120°, γ comes into contact with a different β subunit, and the contact forces that β subunit into the β-empty conformation.

The three β subunits interact in such a way that when one assumes the β-empty conformation, its neighbor to one side *must* assume the β-ADP form, and the other neighbor the β-ATP form. Thus one complete rotation of the γ subunit causes each β subunit to cycle through all three of its possible conformations, and for each rotation, three ATP are synthesized and released from the enzyme surface.

One strong prediction of this binding-change model is that the γ subunit should rotate in one direction when F_oF_1 is synthesizing ATP and in the opposite direction when the enzyme is hydrolyzing ATP. This prediction was confirmed in elegant experiments in the laboratories of Masasuke Yoshida and Kazuhiko Kinosita, Jr. The rotation of γ in a single F_1 molecule was observed microscopically by attaching a long, thin, fluorescent actin polymer to γ and watching it move relative to $\alpha_3\beta_3$ immobilized on a microscope slide, as ATP was hydrolyzed. When the entire F_oF_1 complex (not just F_1) was used in a similar experiment, the entire ring of c subunits rotated with γ (Fig. 19–25). The "shaft" rotated in the predicted direction through 360°. The rotation was not smooth, but occurred in three discrete steps of 120°. As calculated from the known rate of ATP hydrolysis by one F_1 molecule and from the frictional drag on the long actin polymer, the efficiency of this mechanism in converting chemical energy into motion is close to 100%. It is, in Boyer's words, "a splendid molecular machine!"

Chemiosmotic Coupling Allows Nonintegral Stoichiometries of O_2 Consumption and ATP Synthesis

Before the general acceptance of the chemiosmotic model for oxidative phosphorylation, the assumption was that the overall reaction equation would take the following form:

$$x\text{ADP} + x\text{P}_i + \tfrac{1}{2}\text{O}_2 + \text{H}^+ + \text{NADH} \longrightarrow x\text{ATP} + \text{H}_2\text{O} + \text{NAD}^+ \quad (19\text{–}11)$$

with the value of x—sometimes called the **P/O ratio** or the **P/2e^- ratio**—always an integer. When intact mito-

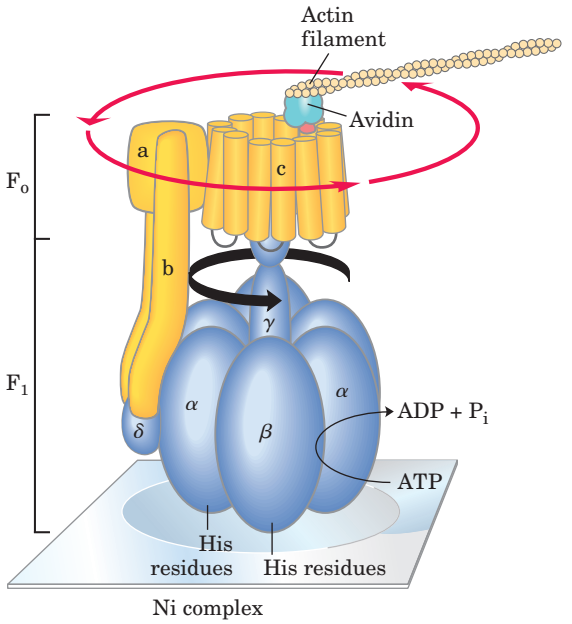

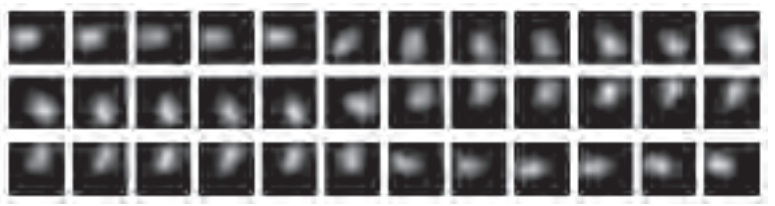

FIGURE 19–25 Rotation of F_o and γ experimentally demonstrated. F_1 genetically engineered to contain a run of His residues adheres tightly to a microscope slide coated with a Ni complex; biotin is covalently attached to a c subunit of F_o. The protein avidin, which binds biotin very tightly, is covalently attached to long filaments of actin labeled with a fluorescent probe. Biotin-avidin binding now attaches the actin filaments to the c subunit. When ATP is provided as substrate for the ATPase activity of F_1, the labeled filament is seen to rotate continuously in one direction, proving that the F_o cylinder of c subunits rotates. In another experiment, a fluorescent actin filament was attached directly to the γ subunit. The series of fluorescence micrographs shows the position of the actin filament at intervals of 133 ms. Note that as the filament rotates, it makes a discrete jump about every eleventh frame. Presumably the cylinder and shaft move as one unit.

chondria are suspended in solution with an oxidizable substrate such as succinate or NADH and are provided with O_2, ATP synthesis is readily measurable, as is the decrease in O_2. Measurement of P/O, however, is complicated by the fact that intact mitochondria consume ATP in many reactions taking place in the matrix, and they consume O_2 for purposes other than oxidative phosphorylation. Most experiments have yielded P/O (ATP to $\frac{1}{2}O_2$) ratios of between 2 and 3 when NADH was the electron donor, and between 1 and 2 when succinate was the donor. Given the assumption that P/O should have an integral value, most experimenters agreed that the P/O ratios must be 3 for NADH and 2 for succinate, and for years those values have appeared in research papers and textbooks.

With introduction of the chemiosmotic paradigm for coupling ATP synthesis to electron transfer, there was no theoretical requirement for P/O to be integral. The relevant questions about stoichiometry became, how many protons are pumped outward by electron transfer from one NADH to O_2, and how many protons must flow inward through the F_oF_1 complex to drive the synthesis of one ATP? The measurement of proton fluxes is technically complicated; the investigator must take into account the buffering capacity of mitochondria, nonproductive leakage of protons across the inner membrane, and use of the proton gradient for functions other than ATP synthesis, such as driving the transport of substrates across the inner mitochondrial membrane (described below). The consensus values for number of protons pumped out per pair of electrons are 10 for NADH and 6 for succinate. The most widely accepted experimental value for number of protons required to drive the synthesis of an ATP molecule is 4, of which 1 is used in transporting P_i, ATP, and ADP across the mitochondrial membrane (see below). If 10 protons are pumped out per NADH and 4 must flow in to produce 1 ATP, the proton-based P/O ratio is 2.5 for NADH as the electron donor and 1.5 (6/4) for succinate. We use the P/O values of 2.5 and 1.5 throughout this book, but the values 3.0 and 2.0 are still common in the biochemical literature. The final word on proton stoichiometry will probably not be written until we know the full details of the F_oF_1 reaction mechanism.

The Proton-Motive Force Energizes Active Transport

Although the primary role of the proton gradient in mitochondria is to furnish energy for the synthesis of ATP, the proton-motive force also drives several transport processes essential to oxidative phosphorylation. The inner mitochondrial membrane is generally impermeable to charged species, but two specific systems transport ADP and P_i into the matrix and ATP out to the cytosol (Fig. 19–26).

The **adenine nucleotide translocase,** integral to the inner membrane, binds ADP^{3-} in the intermembrane space and transports it into the matrix in exchange for an ATP^{4-} molecule simultaneously transported outward (see Fig. 13–1 for the ionic forms of ATP and ADP). Because this antiporter moves four negative charges out for every three moved in, its activity is favored by the

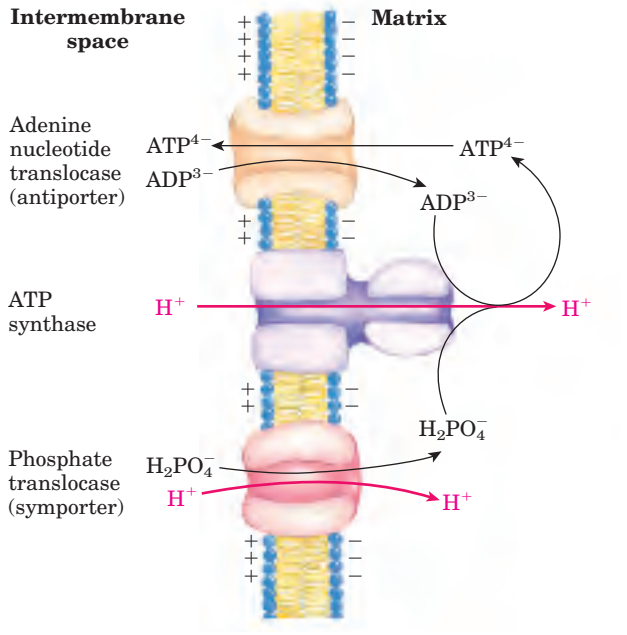

FIGURE 19–26 Adenine nucleotide and phosphate translocases. Transport systems of the inner mitochondrial membrane carry ADP and P_i into the matrix and newly synthesized ATP into the cytosol. The adenine nucleotide translocase is an antiporter; the same protein moves ADP into the matrix and ATP out. The effect of replacing ATP^{4-} with ADP^{3-} is the net efflux of one negative charge, which is favored by the charge difference across the inner membrane (outside positive). At pH 7, P_i is present as both HPO_4^{2-} and $H_2PO_4^-$; the phosphate translocase is specific for $H_2PO_4^-$. There is no net flow of charge during symport of $H_2PO_4^-$ and H^+, but the relatively low proton concentration in the matrix favors the inward movement of H^+. Thus the proton-motive force is responsible both for providing the energy for ATP synthesis and for transporting substrates (ADP and P_i) in and product (ATP) out of the mitochondrial matrix. All three of these transport systems can be isolated as a single membrane-bound complex (ATP synthasome).

transmembrane electrochemical gradient, which gives the matrix a net negative charge; the proton-motive force drives ATP-ADP exchange. Adenine nucleotide translocase is specifically inhibited by atractyloside, a toxic glycoside formed by a species of thistle. If the transport of ADP into and ATP out of mitochondria is inhibited, cytosolic ATP cannot be regenerated from ADP, explaining the toxicity of atractyloside.

A second membrane transport system essential to oxidative phosphorylation is the **phosphate translocase,** which promotes symport of one $H_2PO_4^-$ and one H^+ into the matrix. This transport process, too, is favored by the transmembrane proton gradient (Fig. 19–26). Notice that the process requires movement of one proton from the P to the N side of the inner membrane, consuming some of the energy of electron transfer. A complex of the ATP synthase and both translocases, the **ATP synthasome,** can be isolated from mitochondria by gentle dissection with detergents, suggesting that the functions of these three proteins are very tightly integrated.

Shuttle Systems Indirectly Convey Cytosolic NADH into Mitochondria for Oxidation

The NADH dehydrogenase of the inner mitochondrial membrane of animal cells can accept electrons only from NADH in the matrix. Given that the inner membrane is not permeable to NADH, how can the NADH generated by glycolysis in the cytosol be reoxidized to NAD^+ by O_2 via the respiratory chain? Special shuttle systems carry reducing equivalents from cytosolic NADH into mitochondria by an indirect route. The most active NADH shuttle, which functions in liver, kidney, and heart mitochondria, is the **malate-aspartate shuttle** (Fig. 19–27). The reducing equivalents of cytosolic NADH are first transferred to cytosolic oxaloacetate to yield malate, catalyzed by cytosolic malate dehydrogenase. The malate thus formed passes through the inner membrane via the malate–α-ketoglutarate transporter. Within the matrix the reducing equivalents are passed to NAD^+ by the action of matrix malate dehydrogenase, forming NADH; this NADH can pass electrons directly to the respiratory chain. About 2.5 molecules of ATP are generated as this pair of electrons passes to O_2. Cytosolic oxaloacetate must be regenerated by transamination reactions and the activity of membrane transporters to start another cycle of the shuttle.

Skeletal muscle and brain use a different NADH shuttle, the **glycerol 3-phosphate shuttle** (Fig. 19–28). It differs from the malate-aspartate shuttle in that it delivers the reducing equivalents from NADH to ubiquinone and thus into Complex III, not Complex I (Fig. 19–8), providing only enough energy to synthesize 1.5 ATP molecules per pair of electrons.

The mitochondria of plants have an *externally* oriented NADH dehydrogenase that can transfer electrons directly from cytosolic NADH into the respiratory chain at the level of ubiquinone. Because this pathway bypasses the NADH dehydrogenase of Complex I and the associated proton movement, the yield of ATP from cytosolic NADH is less than that from NADH generated in the matrix (Box 19–1).

SUMMARY 19.2 ATP Synthesis

- The flow of electrons through Complexes I, III, and IV results in pumping of protons across the inner mitochondrial membrane, making the matrix alkaline relative to the intermembrane space. This proton gradient provides the energy (in the form of the proton-motive force) for ATP synthesis from ADP and P_i by ATP synthase (F_oF_1 complex) in the inner membrane.

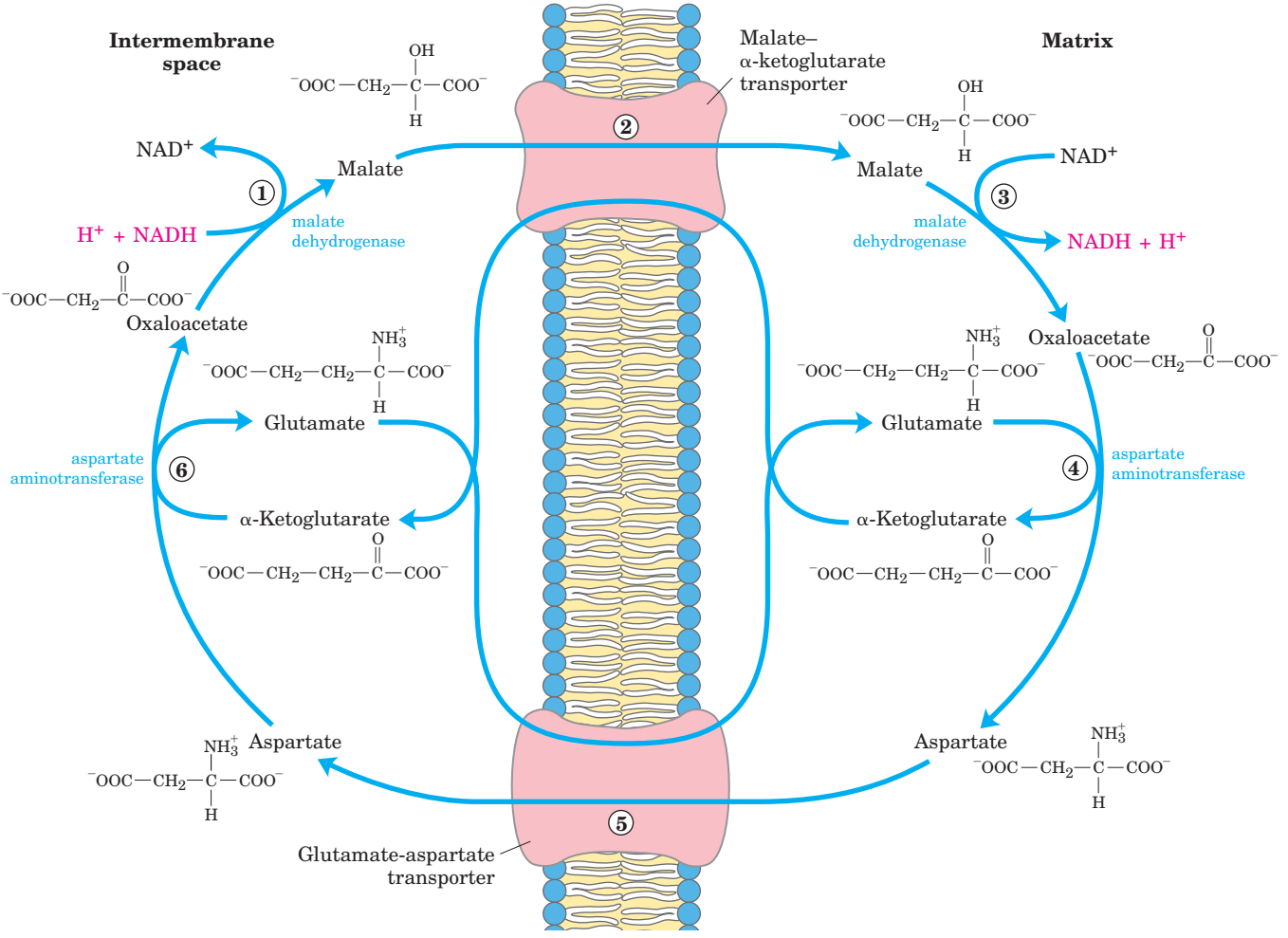

FIGURE 19–27 Malate-aspartate shuttle. This shuttle for transporting reducing equivalents from cytosolic NADH into the mitochondrial matrix is used in liver, kidney, and heart. (1) NADH in the cytosol (intermembrane space) passes two reducing equivalents to oxaloacetate, producing malate. (2) Malate crosses the inner membrane via the malate–α-ketoglutarate transporter. (3) In the matrix, malate passes two reducing equivalents to NAD^+, and the resulting NADH is oxidized by the respiratory chain. The oxaloacetate formed from malate cannot pass directly into the cytosol. (4) It is first transaminated to aspartate, which (5) can leave via the glutamate-aspartate transporter. (6) Oxaloacetate is regenerated in the cytosol, completing the cycle.

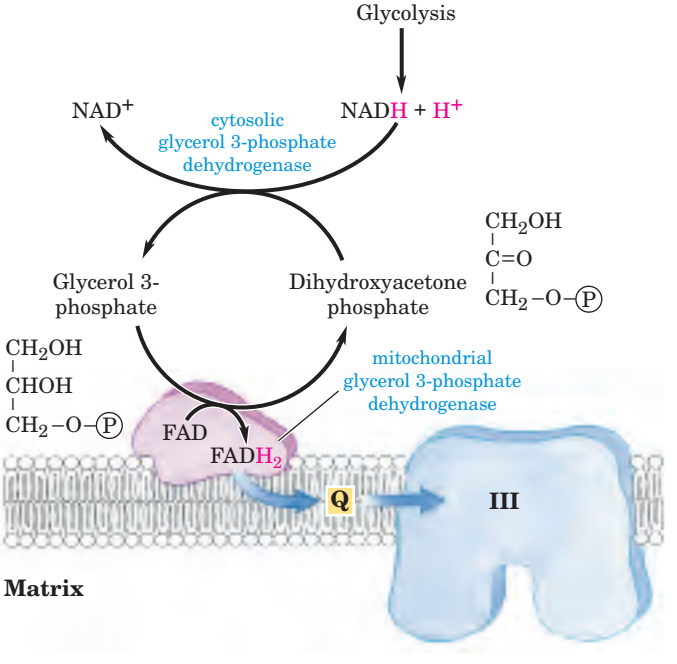

FIGURE 19–28 Glycerol 3-phosphate shuttle. This alternative means of moving reducing equivalents from the cytosol to the mitochondrial matrix operates in skeletal muscle and the brain. In the cytosol, dihydroxyacetone phosphate accepts two reducing equivalents from NADH in a reaction catalyzed by cytosolic glycerol 3-phosphate dehydrogenase. An isozyme of glycerol 3-phosphate dehydrogenase bound to the outer face of the inner membrane then transfers two reducing equivalents from glycerol 3-phosphate in the intermembrane space to ubiquinone. Note that this shuttle does not involve membrane transport systems.

- ATP synthase carries out "rotational catalysis," in which the flow of protons through F_o causes each of three nucleotide-binding sites in F_1 to cycle from (ADP + P_i)–bound to ATP-bound to empty conformations.
- ATP formation on the enzyme requires little energy; the role of the proton-motive force is to push ATP from its binding site on the synthase.
- The ratio of ATP synthesized per $\frac{1}{2}O_2$ reduced to H_2O (the P/O ratio) is about 2.5 when electrons enter the respiratory chain at Complex I, and 1.5 when electrons enter at CoQ.
- Energy conserved in a proton gradient can drive solute transport uphill across a membrane.
- The inner mitochondrial membrane is impermeable to NADH and NAD^+, but NADH equivalents are moved from the cytosol to the matrix by either of two shuttles. NADH equivalents moved in by the malate-aspartate shuttle enter the respiratory chain at Complex I and yield a P/O ratio of 2.5; those moved in by the glycerol 3-phosphate shuttle enter at CoQ and give a P/O ratio of 1.5.

19.3 Regulation of Oxidative Phosphorylation

Oxidative phosphorylation produces most of the ATP made in aerobic cells. Complete oxidation of a molecule of glucose to CO_2 yields 30 or 32 ATP (Table 19–5). By comparison, glycolysis under anaerobic conditions (lactate fermentation) yields only 2 ATP per glucose. Clearly, the evolution of oxidative phosphorylation provided a tremendous increase in the energy efficiency of catabolism. Complete oxidation to CO_2 of the coenzyme A derivative of palmitate (16:0), which also occurs in the mitochondrial matrix, yields 108 ATP per palmitoyl-CoA (see Table 17–1). A similar calculation can be made for the ATP yield from oxidation of each of the amino acids (Chapter 18). Aerobic oxidative pathways that result in electron transfer to O_2 accompanied by oxidative phosphorylation therefore account for the vast majority of the ATP produced in catabolism, so the regulation of ATP production by oxidative phosphorylation to match the cell's fluctuating needs for ATP is absolutely essential.

Oxidative Phosphorylation Is Regulated by Cellular Energy Needs

The rate of respiration (O_2 consumption) in mitochondria is tightly regulated; it is generally limited by the availability of ADP as a substrate for phosphorylation. Dependence of the rate of O_2 consumption on the availability of the P_i acceptor ADP (Fig. 19–18b), the **acceptor control** of respiration, can be remarkable. In some animal tissues, the **acceptor control ratio,** the ratio of the maximal rate of ADP-induced O_2 consumption to the basal rate in the absence of ADP, is at least ten.

The intracellular concentration of ADP is one measure of the energy status of cells. Another, related measure is the **mass-action ratio** of the ATP-ADP system, [ATP]/([ADP][P_i]). Normally this ratio is very high, so the ATP-ADP system is almost fully phosphorylated. When the rate of some energy-requiring process (protein synthesis, for example) increases, the rate of breakdown of ATP to ADP and P_i increases, lowering the mass-action ratio. With more ADP available for oxidative phosphorylation, the rate of respiration increases, causing regeneration of ATP. This continues until the mass-action ratio returns to its normal high level, at which point respiration slows again. The rate of oxidation of cellular fuels is regulated with such sensitivity and precision that the [ATP]/([ADP][P_i]) ratio fluctuates only slightly in most tissues, even during extreme variations in energy demand. In short, ATP is formed only as fast as it is used in energy-requiring cellular activities.

TABLE 19–5 ATP Yield from Complete Oxidation of Glucose

Process	*Direct product*	*Final ATP*
Glycolysis	2 NADH (cytosolic)	3 or 5*
	2 ATP	2
Pyruvate oxidation (two per glucose)	2 NADH (mitochondrial matrix)	5
Acetyl-CoA oxidation in citric acid cycle (two per glucose)	6 NADH (mitochondrial matrix)	15
	2 $FADH_2$	3
	2 ATP or 2 GTP	2
Total yield per glucose		30 or 32

*The number depends on which shuttle system transfers reducing equivalents into the mitochondrion.

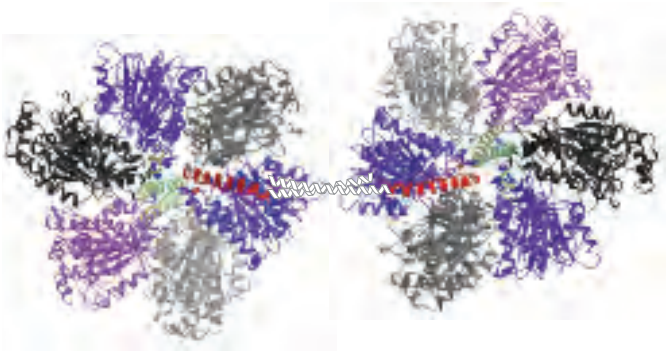

FIGURE 19–29 Structure of bovine F_1-ATPase in a complex with its regulatory protein IF_1. (Derived from PDB ID 1OHH) Two F_1 molecules are viewed here as in Figure 19–23c. The inhibitor IF_1 (red) binds to the $\alpha\beta$ interface of the subunits in the diphosphate (ADP) conformation (αADP and βADP), freezing the two F_1 complexes and thereby blocking ATP hydrolysis (and synthesis). (Parts of IF_1 that failed to resolve in crystals of F_1 are shown in white outline as they occur in crystals of isolated IF_1.) This complex is stable only at the low cytosolic pH characteristic of cells that are producing ATP by glycolysis; when aerobic metabolism resumes, the cytosolic pH rises, the inhibitor is destabilized, and ATP synthase becomes active.

An Inhibitory Protein Prevents ATP Hydrolysis during Ischemia

We have already encountered ATP synthase as an ATP-driven proton pump (see Fig. 11–39; Table 11–3), catalyzing the reverse of ATP synthesis. When a cell is ischemic (deprived of oxygen), as in a heart attack or stroke, electron transfer to oxygen ceases, and so does the pumping of protons. The proton-motive force soon collapses. Under these conditions, the ATP synthase could operate in reverse, hydrolyzing ATP to pump protons outward and causing a disastrous drop in ATP levels. This is prevented by a small (84 amino acids) protein inhibitor, IF_1, which simultaneously binds to two ATP synthase molecules, inhibiting their ATPase activity (Fig. 19–29). IF_1 is inhibitory only in its dimeric form, which is favored at pH lower than 6.5. In a cell starved for oxygen, the main source of ATP becomes glycolysis, and the pyruvic or lactic acid thus formed lowers the pH in the cytosol and the mitochondrial matrix. This favors IF_1 dimerization, leading to inhibition of the ATPase activity of ATP synthase, thereby preventing wasteful hydrolysis of ATP. When aerobic metabolism resumes, production of pyruvic acid slows, the pH of the cytosol rises, the IF_1 dimer is destabilized, and the inhibition of ATP synthase is lifted.

Uncoupled Mitochondria in Brown Fat Produce Heat

There is a remarkable and instructive exception to the general rule that respiration slows when the ATP supply is adequate. Most newborn mammals, including humans, have a type of adipose tissue called **brown fat** in which fuel oxidation serves not to produce ATP but to generate heat to keep the newborn warm. This specialized adipose tissue is brown because of the presence of large numbers of mitochondria and thus large amounts of cytochromes, whose heme groups are strong absorbers of visible light.

The mitochondria of brown fat are like those of other mammalian cells in all respects, except that they have a unique protein in their inner membrane. **Thermogenin,** also called the **uncoupling protein** (Table 19–4), provides a path for protons to return to the matrix without passing through the F_oF_1 complex (Fig. 19–30).

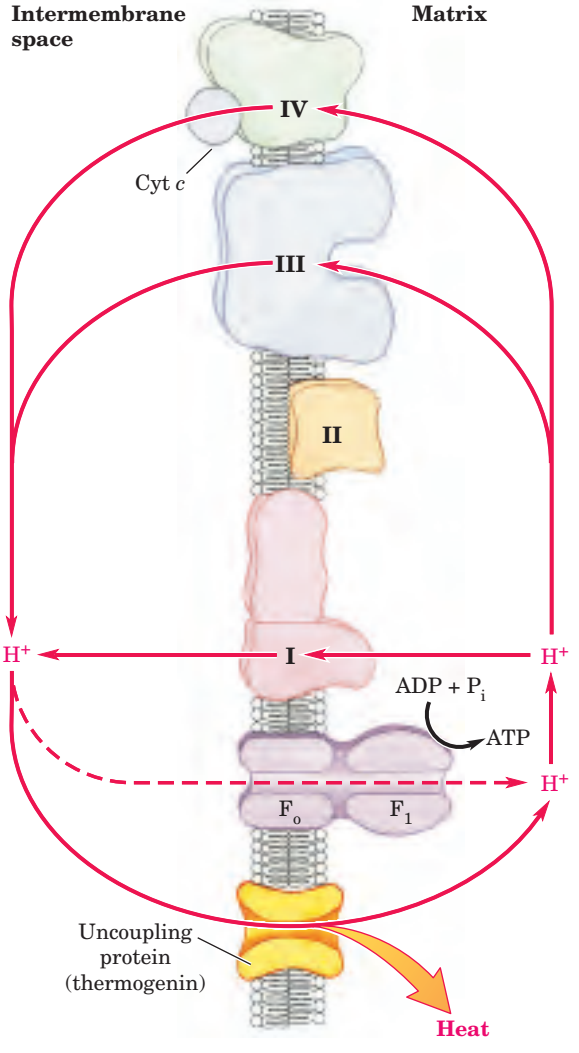

FIGURE 19–30 Heat generation by uncoupled mitochondria. The uncoupling protein (thermogenin) of brown fat mitochondria, by providing an alternative route for protons to reenter the mitochondrial matrix, causes the energy conserved by proton pumping to be dissipated as heat.

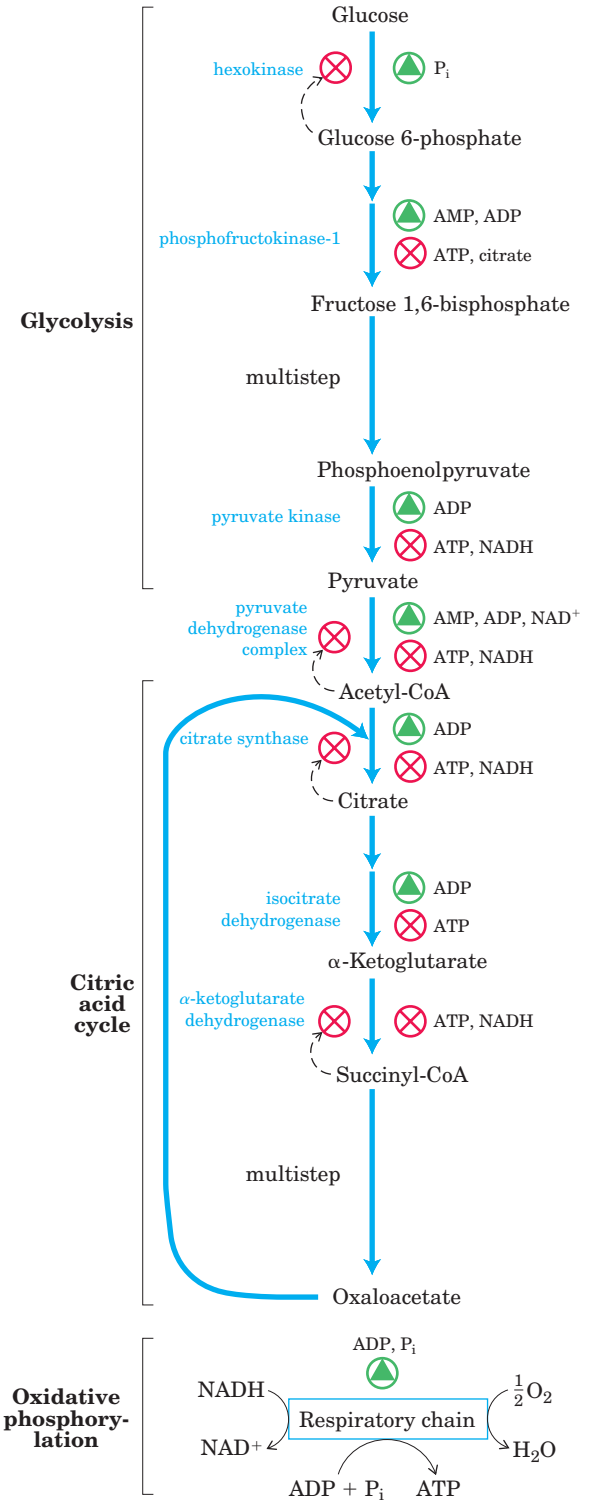

FIGURE 19–31 Regulation of the ATP-producing pathways. This diagram shows the interlocking regulation of glycolysis, pyruvate oxidation, the citric acid cycle, and oxidative phosphorylation by the relative concentrations of ATP, ADP, and AMP, and by NADH. High [ATP] (or low [ADP] and [AMP]) produces low rates of glycolysis, pyruvate oxidation, acetate oxidation via the citric acid cycle, and oxidative phosphorylation. All four pathways are accelerated when the use of ATP and the formation of ADP, AMP, and P_i increase. The interlocking of glycolysis and the citric acid cycle by citrate, which inhibits glycolysis, supplements the action of the adenine nucleotide system. In addition, increased levels of NADH and acetyl-CoA also inhibit the oxidation of pyruvate to acetyl-CoA, and a high [NADH]/[NAD^+] ratio inhibits the dehydrogenase reactions of the citric acid cycle (see Fig. 16–18).

ATP-Producing Pathways Are Coordinately Regulated

The major catabolic pathways have interlocking and concerted regulatory mechanisms that allow them to function together in an economical and self-regulating manner to produce ATP and biosynthetic precursors. The relative concentrations of ATP and ADP control not only the rates of electron transfer and oxidative phosphorylation but also the rates of the citric acid cycle, pyruvate oxidation, and glycolysis (Fig. 19–31). Whenever ATP consumption increases, the rate of electron transfer and oxidative phosphorylation increases. Simultaneously, the rate of pyruvate oxidation via the citric acid cycle increases, increasing the flow of electrons into the respiratory chain. These events can in turn evoke an increase in the rate of glycolysis, increasing the rate of pyruvate formation. When conversion of ADP to ATP lowers the ADP concentration, acceptor control slows electron transfer and thus oxidative phosphorylation. Glycolysis and the citric acid cycle are also slowed, because ATP is an allosteric inhibitor of the glycolytic enzyme phosphofructokinase-1 (see Fig. 15–18) and of pyruvate dehydrogenase (see Fig. 16–18).

Phosphofructokinase-1 is also inhibited by citrate, the first intermediate of the citric acid cycle. When the cycle is "idling," citrate accumulates within mitochondria, then spills into the cytosol. When the concentrations of both ATP and citrate rise, they produce a concerted allosteric inhibition of phosphofructokinase-1 that is greater than the sum of their individual effects, slowing glycolysis.

As a result of this short-circuiting of protons, the energy of oxidation is not conserved by ATP formation but is dissipated as heat, which contributes to maintaining the body temperature of the newborn. Hibernating animals also depend on uncoupled mitochondria of brown fat to generate heat during their long dormancy (see Box 17–1).

SUMMARY 19.3 Regulation of Oxidative Phosphorylation

- Oxidative phosphorylation is regulated by cellular energy demands. The intracellular [ADP] and the mass-action ratio [ATP]/([ADP][P_i]) are measures of a cell's energy status.